RECOMBINANT ANTI-TENASCIN ANTIBODY CONSTRUCTS

Final Progress Report
For the Period 5/1/1995-11/30/2005

Michael R. Zalutsky

Duke University Medical Center
Durham, North Carolina, 27710

August 2006

Prepared for

A.   SCOPE AND SPECIFIC AIMS

The development of hybridoma technology some thirty years ago rekindled interest in exploiting the specificity of the antigen-antibody interaction to target radioactivity to tumor for diagnostic and therapeutic applications. Despite widespread efforts, radiolabeled monoclonal antibodies (MAbs) have not had a significant impact on the clinical management of cancer patients. The marginal utility of labeled MAbs can be attributed to multiple factors, including those unrelated to antigen specificity such as Fc receptor binding, vascular clearance and tumor penetration. Increasing the utility of labeled MAbs will require optimization of these parameters in concert with improvements in MAb specificity and radiolabeling. Our approach will employ DNA recombinant technology to generate genetically engineered MAb-based constructs and evaluate their potential utility for oncologic nuclear medicine. **It was the central hypothesis of this proposal that the general framework of these molecules will be a critical factor in determining their utility with radionuclides and that the ideal molecular form will also depend on the nature of the radionuclide, labeling method and route of administration.**

Our work plan was focuseded on MAb-based constructs reactive with tenascin, a polymorphic extracellular matrix glycoprotein found in gliomas, neuroblastomas, melanomas, as well as prostate and breast carcinomas. Variable regions will be derived from murine 81C6 MAb, which binds to the alternatively spliced fibronectin type III domain 6 of the tenascin molecule. Our extensive preclinical and clinical experience using murine 81C6 can serve as a valuable reference point for the proposed studies. Moreover, we had obtained promising therapeutic responses with ^{131}I-labeled 81C6 in patients with cystic gliomas, surgically-created glioma resection cavities and neoplastic meningitis.

This research proposal sought to identify the optimal antibody-based constructs for use with radionuclides. Experiments focused on radioiodine nuclides, the α-emitter ^{211}At and the positron emitter ^{18}F in order to exploit novel radiohalogenation strategies developed in our laboratory. The first goal was to select a construct for use with longer half-life nuclides, such as ^{131}I, which can be best exploited in applications where slow blood clearance and limited tumor penetration are not major problems. For this task, chimeric MAbs with constant regions from the four different human IgG classes were constructed, as were molecules with domain deletions engineered to alter pharmacokinetics. Our preliminary data suggested that use of the IgG_2 constant region offers significant advantages for radionuclide applications. We also proposed the investigation of sFv monomers and dimers because their rapid normal tissue clearance and tumor penetration should be compatible with shorter half-life nuclides such as ^{18}F and ^{211}At. The specific aims proposed for the initial grant period in the original application were:

Specific Aim 1a. To construct and express human/mouse chimeric MAbs for 81C6 with IgG_1, IgG_3 and IgG_4 constant regions.

Specific Aim 2a. To develop human/mouse chimeric 81C6 with domain deletions or alterations in glycosylation sites. Engineered immunoglobulins with CH_2 domain deletion should offer more rapid blood clearance similar to that of F(ab')$_2$ but with enhanced stability.

Specific Aim 3a. To engineer monovalent and divalent sFv recombinant proteins using variable region cDNA sequences for 81C6. Heavy- and light-chain cDNA for 81C6 will be cloned via the

2

polymerase chain reaction and will be joined via a linker oligonucleotide sequence. Expression in *Escherichia coli* will be optimized with strong promoters. Initially, renaturation and refolding will be directed towards periplasmic places in *E. coli.*

Specific Aim 4a. To label these 81C6 MAb-based constructs with ^{131}I, ^{211}At and ^{18}F using *N*-succinimidyl [^{131}I]iodo-, [^{211}At]astato- and [^{18}F]fluorobenzoate, respectively, with retention of immunoreactivity and affinity.

Specific Aim 5a. To evaluate the tissue distribution of these labeled molecules in normal mice and athymic rodents with subcutaneous, intracerebral and neoplastic meningitis xenograft models.

Specific Aim 6a. To determine the therapeutic efficacy in athymic rodent xenograft models of promising candidate molecules labeled at equitoxic doses of ^{131}I and ^{211}At.

During the first grant period, our efforts were focused on the evaluation of a chimeric mAb containing murine 81C6 variable regions and human IgG$_2$ constant regions. Based on the excellent tumor targeting and stability of this molecule in animal models, we submitted and obtained an Investigational New Drug Application to permit its evaluation in patients. In the second grant period, we focused on the development and evaluation of anti-tenascin constructs with optimal properties (mass, valency, domain structure, normal tissue clearance, tumor uptake kinetics and penetration) for use with short half-life radionuclides. Astatine-211 is a 7.2-hr α-particle emitter of considerable promise for certain radioimmunotherapeutic applications, 13-hr ^{123}I has excellent properties for single photon emission computed tomography, and 1.8-hr ^{18}F is the most frequently used radionuclide in clinical positron emission tomography. The specific aims proposed for the second grant period were:

Specific Aim 1b. To generate higher affinity anti-tenascin constructs via phage display technology. These studies will utilize a peptide immunogen based on the amino acid sequence and three-dimensional conformation of the epitope to which 81C6 binds on domain 12 of the alternatively spliced fibronectin type III repeat on the tenascin molecule.

Specific Aim 2b. To construct a high-affinity, monovalent, single-chain anti-tenascin mAb construct with V_H and V_L domains connected by a peptide linker (scFv), pair of disulfide bonds (dsFv), or both (scdsFv).

Specific Aim 3b. To construct a bioengineered, bivalent anti-tenascin mAb construct (either an scFv or dsFv dimer, an scFv-CH$_3$ minibody, or CH$_2$ domain deletion construct) with appropriate properties for radioimmunotargeting.

Specific Aim 4b. To determine whether the targeting of these anti-tenascin constructs can be enhanced by minimizing radiolabel substitution on amino acid residues critical for antigen recognition and tertiary structure. This will be accomplished by either addition of a lysine rich peptide tail or site-directed mutagenesis of lysine residues in CDR regions.

Specific Aim 5b. To label the best monovalent and divalent anti-tenascin constructs with ^{211}At, ^{18}F and radioiodine nuclides, with maximum retention of immunoreactivity, affinity and stability.

Specific Aim 6b. To evaluate the potential utility of the best radiohalogenated anti-tenascin monovalent and divalent constructs for diagnostic and therapeutic applications by determining their a) paired-label tissue distribution in normal mice and athymic rodents bearing subcutaneous, intracerebral and neoplastic meningitis xenografts; b) projected radiation dosimetry from tissue distribution and quantitative autoradiography; and c) therapeutic potential in comparison with equitoxic doses of ^{131}I- and ^{211}At-labeled anti-tenascin mAbs and fragments.

In the final grant period, we further refined our hypothesis that a multivalent scFv with high *in vivo* stability and affinity for tenascin will increase the therapeutic efficacy of ^{211}At due to its more rapid tumor penetration and clearance from normal tissues. Our goal was to increase the clinical potential of radiolabeled anti-tenascin constructs and investigate these hypotheses, and we proposed the following specific aims:

Specific Aim 1c: To construct a bioengineered, bivalent, anti-tenascin mAb fragment containing murine 81C6 variable regions and the human IgG$_2$ hinge region. Our first candidate will be the CH$_2$ domain deletion construct.

Specific Aim 2c: To construct a single-chain Fv multimer with adequate stability, affinity and immunoreactivity for use in tandem with ^{211}At for therapy and ^{18}F for imaging. Variables to be investigated include nature of the V_L-V_H linker, scFv disulfide stabilization, and link between the scFv monomeric units.

Specific Aim 3c: To generate higher affinity scFv constructs reactive with the alternatively spliced fibronectin type III repeats CD of the tenascin molecule via phage display technology and site-directed mutagenesis.

Specific Aim 4c: To label promising anti-tenascin constructs with radioiodine, ^{211}At, and ^{18}F and evaluate their potential as radiodiagnostic and radiotherapeutic agents. The proposed studies include: characterization of affinity and immunoreactivity after labeling; evaluation of tissue distribution and projected dosimetry in normal mice, and athymic rodents with subcutaneous, intracranial and neoplastic meningitis xenografts; investigation of the nature of low and high molecular weight labeled catabolites generated in mice; and assessment of cytotoxicity *in vitro* and *in vivo* models of human glioma, and possibly, other tenascin expressing tumors.

Specific Aim 5c: To investigate strategies for labeling scFv monomers and dimers which will minimize retention of the radiohalogen in the kidneys through the use of negatively charged templates.

B.   RESULTS

1Radioiodinated Chimeric Anti-Tenascin mAb 81C6: Characterization in Comparison with its Murine Parent

This anti-tenacin chimeric mAb was produced by genomic cloning, and consisted of the variable region genes of murine 81C6 combined with human IgG$_2$ constant region domains. The reactivity of chimeric 81C6 with recombinant tenascin fragments was identical to that observed for

murine 81C6; binding was limited to the fragment containing fibronectin III domains 6-12. In addition, the affinity constant for the binding of radioiodinated chimeric and murine 81C6 to human glioma cells was virtually identical. Nonetheless, initial tissue distribution studies in athymic mice bearing D-54 MG human glioma xenografts indicated unexpected differences in the *in vivo* behavior of the two mAbs: the chimeric molecule (labeled using Iodogen) exhibited more than two-fold higher tumor uptake in both subcutaneous and intracranial xenografts and in some cases, also was retained to a greater degree in normal tissues.

Several experiments were performed in order to explore the nature of the differences in the *in vivo* behavior of chimeric and murine 81C6. The tumor localization of chimeric 81C6 was compared with that of a nonspecific human IgG$_2$ mAb to determine whether the increased uptake of chimeric 81C6 in these xenografts was due to specific processes. Additional investigations were performed with chimeric and murine 81C6 labeled with *N*-succinimidyl 3-[$^{125/131}$I]iodobenzoate (SIB) because previous studies demonstrated that murine 81C6 labeled by this method exhibited superior tumor localization and inertness to deiodination compared with mAb labeled using Iodogen. Our goals were to determine whether higher tumor uptake of chimeric compared with murine 81C6 also could be achieved using SIB, and whether the tumor delivery advantage of the chimeric mAb and the SIB labeling method were additive.

In the first tissue distribution experiment, animals received ^{125}I-labeled chimeric 81C6 and ^{131}I-labeled chimeric TPS3.2, a human IgG$_2$ with no known specificity for glioma. The localization index, defined as the ratio of specific to control mAb in tissue normalized to the ratio of specific to control mAb measured simultaneously in blood, was calculated to determine the specificity of chimeric 81C6 tumor accumulation. Chimeric 81C6 exhibited specific tumor uptake as early as 12 hr after injection with a localization index of 3.3 ± 0.4. The tumor localization index for chimeric 81C6 continued to rise throughout the course of the experiment, reaching 127 ± 36 on Day 16. These tumor localization indices were higher than those reported previously for murine 81C6 in this xenograft model.

In the next experiment, the biodistribution of chimeric and murine 81C6 were compared after labeling using the SIB reagent. Blood pool activity of the mAbs was similar at early time points but by Day 2, there was nearly a twofold difference (chimeric, $14.6 \pm 1.8\%$ ID/g; murine $8.0 \pm 2.0\%$ ID/g; $P < 0.05$). By Day 8, blood pool activity of chimeric 81C6 was about 8 times that of murine 81C6 (chimeric $3.5 \pm 1.8\%$ ID/g; murine, $0.45 \pm 0.20\%$ ID/g; $P < 0.05$). The tumor accumulation of both ^{125}I-labeled chimeric 81C6 and ^{131}I-labeled murine 81C6 reached a maximum on Day 2, with a twofold uptake advantage observed for the chimeric mAb ($49.3 \pm 16.1\%$ ID/g *vs.* $29.3 \pm 1.3\%$ ID/g). Chimeric mAb had a fourfold greater tumor retention than murine mAb on Days 8, 10 and 16. Thyroid accumulation (an *in vivo* indicator of deiodination) was 0.1% of the injected dose or less at all time points for both mAbs. In general, the normal tissue accumulation of chimeric 81C6 was greater than that of murine 81C6 with the differences increasing with time.

We next investigated a number of factors which might contribute to the different *in vivo* behavior of chimeric and murine 81C6. First, the sites of labeling on the two mAbs probably are different since most of the tyrosines and lysines reside in the constant regions. With the Iodogen method, percent heavy chain labeling observed for chimeric (83%) and murine 81C6 (82%) were almost identical. In contrast, when the SIB method was used, 72% of the label was found on the heavy chain for murine 81C6 compared with 56% for chimeric 81C6. Because the uptake of

5

chimeric 81C6 was greater than its murine parent not only in tumor but also in many normal tissues, differences in pI between the two IgG could be relevant since the pI of mAbs has been shown to influence its tissue distribution. After radioiodination using Iodogen, the isoelectric point of chimeric 81C6 was 0.5-0.9 pI units higher than that of murine 81C6. The greater positive charge of the chimeric mAb is consistent with its higher tissue retention; however, it is not clear whether the magnitude of the pI difference would be sufficient to account for the observed tissue uptake patterns. In addition, the pI of chimeric 81C6 labeled using Iodogen was 7.4-7.6 and the primary bands with SIB were of similar pI. Because proteins are least soluble at their pI, it might be possible that the proximity of the pI of chimeric 81C6 to physiological pH could contribute to its increased tissue deposition relative to murine 81C6 and nonspecific control mAbs, all of which have pI dissimilar to pH 7.4.

The third paired-label study directly compared the tumor and normal tissue retention of chimeric 81C6 labeled using Iodogen and SIB in order to determine whether the tumor uptake advantage associated with SIB labeling and use of the chimeric were additive. Blood clearance of ^{125}I-labeled (Iodogen) and ^{131}I-labeled (SIB) chimeric 81C6 were virtually identical. Labeling chimeric 81C6 using SIB reduced thyroid uptake of radioiodine significantly. The ratio of the % ID in thyroid for MAb labeled using Iodogen to that for mAb labeled using SIB ranged from 4.6 ± 3.1 at 12 hr to 17.4 ± 6.4 at 4 days. No other significant differences in normal tissue localization were observed between the two labeling methods. Modest improvements in tumor retention were observed for mAb labeled using SIB on Days 6 (10 ± 6%), 10 (19 ± 6%) and 16 (25 ± 15%), but differences were not significant by paired t-test at other time points. With the exception of stomach, tumor-to-normal tissue ratios for mAb labeled using Iodogen and SIB were nearly identical from 12 hr to 4 days; however, slightly higher ratios were observed at later time points for chimeric 81C6 labeled using SIB. A more pronounced advantage was seen for SIB in stomach, reaching a factor of 2 by 6 days after injection.

Because an advantage of SIB is the creation of an iodination site that minimizes recognition by endogenous deiodinases, the lack of major improvement in tumor uptake of chimeric 81C6 might be related to a low susceptibility of this mAb to deiodination. This possibility is supported by the fact that with chimeric 81C6, SIB labeling lowered thyroid by only about 5- to 17-fold compared with a factor of as much as 108 for murine mAb. In addition, the thyroid uptake of chimeric mAb was 2 to 3 times lower than that of murine mAb in two separate paired-label experiments comparing the tissue distribution of chimeric and murine 81C6 labeled using Iodogen. Taken together, these results suggest that there are differences in murine and chimeric mAb catabolism which, depending on the labeling method, may or may not result in differences in deiodination.

Catabolism of Radioiodinated Chimeric and Murine 81C6 mAbs

Recently, we have completed an investigation comparing the catabolism of chimeric and murine 81C6 labeled using Iodogen in athymic mice bearing subcutaneous D-54 MG glioma xenografts. Prior to injection, both mAbs were greater than 99% trichloroacetic acid (TCA) precipitable and moved as a single band on SDS-PAGE with a molecular weight corresponding to IgG. Total body retention of ^{131}I(-labeled chimeric mAb) was significantly higher than that of ^{125}I (-labeled murine mAb) over the first 72 hr and a corresponding increase in the urinary excretion of TCA-soluble ^{125}I in the urine was seen. Tumor, liver, spleen and kidney were homogenized to

6

examine the nature of the radioactive species in these tissues as well as in the blood. Tissue homogenate supernatant were analyzed initially for TCA precipitability to determine the amount of low molecular weight catabolites. The percentage TCA-soluble counts was less than 10% for all tissues at all time points but generally were lower for chimeric 81C6. For example, the TCA-soluble percentages for murine mAb in liver, spleen, kidney, blood and tumor were 3.1 ± 0.6, 4.7 ± 0.4, 3.0 ± 0.6, 0.9 ± 0.1 and $9.3 \pm 4.6\%$, respectively, while for chimeric 81C6, these percentages were significantly lower ($P < 0.05$): 0.8 ± 0.3, 1.7 ± 0.6, 0.9 ± 0.2, 0.5 ± 0.1, and $1.5 \pm 0.5\%$. These results suggest that radioiodinated chimeric 81C6 is less susceptible to catabolism than its murine counterpart.

The nature of the higher molecular weight labeled catabolites generated *in vivo* was investigated using sodium dodecyl sulfate polyacrylamide gel electrophoresis (SDS-PAGE). Images of the gels were obtained and the radioactivity in the bands quantified using a phosphor image analysis system. Dried gels were exposed to a phosphor screen (Kodak) for 48 hr. The screen was scanned using a Storm 860 Phosphorimager (Molecular Dynamics) and the resultant image was analyzed using the ImageQuant analysis program (Molecular Dynamics). The profiles of labeled catabolites found in tumor 24 and 144 hr after injection of the labeled mAbs showed that at 24 hr, approximately 52% of ^{131}I(-labeled chimeric mAb) activity in the tumor homogenate had a molecular weight corresponding to intact IgG compared with 38% for ^{125}I(-labeled murine mAb). Even more striking differences were observed at 144 hr at which time the percentage of tumor associated radioiodine activity present as intact mAb was more than twice as high for chimeric compared with murine 81C6. Similar trends were observed in normal tissues. The molecular weight distribution of radioiodine activity at 24 hr for liver, spleen, kidney and blood showed with the exception of blood, a higher percentage of radioiodine activity was present as intact IgG for the chimeric mAb. A substantial fraction of radioactivity for murine but not chimeric mAb was present In both tumor and normal organs as an as yet unidentified 70-90 kD catabolite. One possibility is that this molecule was generated by the cleavage of inter-chain disulfide bonds. In summary, these results confirm that chimeric 81C6 is more resistant to *in vivo* catabolism than its murine counterpart. It is likely that this difference contributes to the higher tumor and normal tissue retention of this chimeric mAb.

Enhanced Delivery of Radioiodinated Chimeric 81C6 to Subcutaneous Glioma Xenografts by Local Hyperthermia

A number of laboratories including our own have demonstrated that local hyperthermia can improve the tumor accumulation of mAbs and mAb fragments reactive with cell surface antigens. Because hyperthermia can modulate the expression of cell-surface antigens, typically resulting in an initial decrease in antigen expression, a mAb directed against a matrix antigen such as tenascin might be preferable. The effect of local hyperthermia on the tissue distribution of ^{125}I-labeled chimeric 81C6 and ^{131}I-labeled chimeric TPS3.2 nonspecific control was investigated. The D-54 MG subcutaneous glioma xenograft was administered hyperthermia by immersion of the tumor-bearing leg in a circulating water bath. Administration of ^{125}I-labeled chimeric 81C6 concomitantly with a 4 hr, 41.8°C local hyperthermia treatment resulted in a significant ($P < 0.005$) increase in mAb tumor uptake immediately post-heating from a median of 12.0% ID/g of tumor in normothermic mice to 42.0% ID/g in mice receiving local hyperthermia. The increased level of tumor uptake persisted in the heated tumors over the first 48 hr after injection, at which time 69.6% I D/g (*vs.* 36.6% ID/g for normothermic mice) localized in tumor. Hyperthermia also increased the

specificity of tumor localization at 4 hr as reflected by the increase in localization index from 2.21 (normothermic) to 3.35 (heated, $P < 0.005$). In addition, heating increased the tumor-to-blood ratio of chimeric ^{125}I-labeled 81C6 more than 7-fold at 4 hr post-injection. The rate of tumor uptake also was dramatically improved, with 60 and 90% of maximum accumulation achieved by 4 and 24 hr, respectively, in the hyperthermia-treated mice. In comparison, control mice reached only 31 and 69% of their maximum tumor uptake at those time points. In summary, local hyperthermia enhanced both the absolute level and rate of tumor uptake as well as tumor-to-normal tissue ratios for chimeric 81C6. This approach should facilitate clinical application of radionuclides with shorter half-lives, such as ^{211}At, for radioimmunotherapy.

Tissue Distribution and Radiation Dosimetry of ^{211}At-Labeled Chimeric 81C6

This study was performed in anticipation of clinical evaluation of ^{211}At-labeled chimeric 81C6 in patients with neoplastic meningitis, cystic glioma, and surgically created glioma resection cavities. The biodistribution of ^{211}At-labeled chimeric 81C6 in mice bearing D-54 MG subcutaneous glioma xenografts was determined and compared to that obtained when labeled with ^{131}I. These data were used to estimate radiation absorbed doses in humans for ^{211}At-labeled chimeric 81C6 administered by both the intravenous and intrathecal route. Mice were injected intravenously with ^{211}At-labeled chimeric 81C6 (2 µCi, 1 µCi/µg) and ^{131}I-labeled chimeric 81C6 (1.5 µCi, 0.8 µCi/µg) and groups of 5 animals were killed by halothane overdose at 30 min and 2, 4, 8, 16, 24, and 48 hr.

Accumulation of ^{211}At-labeled chimeric 81C6 in tumor increased from 4.5 ± 0.8% ID/g at 30 min to 20.0 ± 3.8% ID/g at 16 hr and remained constant thereafter. The uptake of ^{131}I-labeled chimeric 81C6 in D-54 MG xenografts was not significantly different at the 30 min through 8 hr time points; however, ^{131}I tumor uptake values were 10-39% higher ($P < 0.05$ by paired t-test) than those for ^{211}At from 16 hr to 48 hr. Nonetheless, the cumulative activity in tumor per mCi of ^{211}At-labeled chimeric 81C6 was calculated to be 1405 ± 132 µCi-hr/g, a value about 8% lower than that which would have been predicted using the ^{131}I biodistribution data (1514 ± 106 µCi-hr/g). These results suggest that serial tumor imaging with a radioiodinated mAb could provide a reasonable estimate of cumulative activity concentrations that would be obtained when the mAb was labeled with ^{211}At.

Activity concentrations of ^{211}At-labeled chimeric 81C6 in the athymic mouse were extrapolated to humans using the %-kg/g method. The extrapolated data were fit to one- or two-compartment exponential functions, and residence times for source organs were obtained by integrating the exponential functions to infinite time, including the radioactive decay of ^{211}At, and assuming that the biological clearances observed continued beyond the end of the data sets. Residence times were entered into a version of the MIRDOSE 3.1 software program modified to calculate the dose from α-emissions. For all organs, a radiation weighting factor of 5 was applied to the α-emissions, and a radiation weighting factor of 1 was applied to all photon and electrons. Radiation dosimetry calculations were performed for intravenously administered mAb, mAb confined to the CSF after intrathecal administration, and for varying degrees of leakage of activity from the CSF into the vascular compartment.

Table 2. Radiation on Dose Estimates for ^{211}At-LabeledChimeric 81C6 Antibody: Effect of Leakage from Non-Intravenous Injection Site for 5mCi Dose

Organ	Radiation Dose (rem)			
	1.5%[*]	5%	10%	15%
Brain	0.14	0.45	0.91	1.36
Small Intestine	0.62	2.07	4.15	6.22
Stomach	0.62	2.07	4.15	6.22
Heart Wall	1.50	5.01	10.02	15.03
Kidneys	1.20	3.99	7.98	11.97
Liver	1.14	3.79	7.57	11.36
Lungs	2.92	9.75	19.49	29.24
Red Marrow	1.54	5.12	10.24	15.36
Spleen	0.95	3.18	6.35	9.53
Thyroid	0.60	2.01	4.02	6.03
Bladder Wall	0.66	2.20	4.39	6.59

[*]Percentage Leakage

In patients, the maximum percentage of ^{131}I-labeled murine 81C6 found in the blood pool during the first 3 days after intrathecal injection has ranged between 3 and 6%. If one assumes similar pharmacokinetic behavior in humans for [211]At-labeled chimeric 81C6, this leakage level would correspond to a maximum of only 1.5% of the administered [211]At activity due to the 7.2-hr half life of this radionuclide. Based on our dosimetry calculations published in **[4]**, and a projected initial clinical dose of 5 mCi of [211]At-labeled chimeric 81C6, we have estimated the dosimetry which would result if 1.5% to 15% of the [211]At activity leaked from a non-intravenous injection site into the vascular space **(Table 2)**. These calculations indicate that the lungs and red marrow are the dose-limiting critical organs and that the extent of leakage of [211]At into the vascular compartment will have a major impact on normal organ radiation doses. Even if the leakage of [211]At-labeled chimeric 81C6 were 10 times higher than observed in patients with ^{131}I-labeled murine 81C6, the dose received by red marrow and lungs from 5 mCi of [211]At-labeled mAb would be low, about 15 and 29 rem, respectively. These normal organ doses are lower than those reported for clinical radioimmunotherapy trials with ^{131}I-labeled mAbs.

Cytotoxicity of [211]At-Labeled Chimeric 81C6 for Human Glioma Cells in Microcolonies and Spheroids

The *in vitro* cytotoxicity of [211]At-labeled chimeric 81C6 was investigated in microcolonies of the D-247 MG human glioma and SK-MEL-28 human melanoma cell lines. Microcolony models were used in an attempt to simulate the tumor geometry characteristic of neoplastic meningitis. D-247 MG microcolonies contained an average of 16 cells at the time of treatment with an average distance between cells of 22 μm. Cell and nuclear diameters were 18.5 μm and 9.5 μm, respectively. SK-MEL-28 cells grew in closely packed colonies consisting of an average of 25 cells. The average diameter of the cells and cell nuclei was 20.3 μm and 10.7 μm, respectively. Microcolonies of both cell lines were incubated for 1 hr with varied activity

concentrations of ^{211}At-labeled chimeric 81C6, washed to remove unbound activity, and incubated for an additional 23 hr. In parallel, the uptake and washout kinetics of labeled mAb in these microcolonies was determined to provide cumulative activity information for microdosimetry calculations. These calculations were performed by Gamal Akabani, Ph.D., who joined the faculty in the Department of Radiology this year. Monte Carlo transport of α-particles was used to assess the single-event frequency distribution $f_1(z)$ based on the monolayer arrangements described above.

The activity concentrations reducing cell survival to 37% (A_{37} with 95% confidence interval) for ^{211}At-labeled chimeric 81C6 were determined by regression analysis to be 56.6(50.0-64.7) kBq/ml and 61.1(48.2-83.4) kBq/ml for the D-247 MG and SK-MEL-28 microcolonies, respectively. Decays were assumed to occur in the cell matrix and the cell nucleus was considered as the target. For D-247 MG microcolonies, the calculated average absorbed dose, D_{37}, was 0.27 Gy, the microsimetric cell sensitivity z_0 parameter was 0.10 Gy, and the corresponding number of hits to the cell nucleus at 37% survival, $\langle n \rangle_{37}$, was 1.16. For SK-MEL-28 microcolonies, D_{37} was 0.27 Gy, z_0 was 0.14 Gy, and $\langle n \rangle_{37}$ was 1.54. Differences in z_0 were large, reflecting differences in specific-energy distribution resultant from dissimilar geometrical configurations of the two microcolony models. With both cell lines, reduction in survival to 37% required only 1-2 hits to the cell nucleus, confirming the exquisite cytotoxicity of ^{211}At α-particles.

Recently, we have investigated the cytotoxicity of ^{211}At-labeled chimeric 81C6 in the D-247 MG tumor spheroid model. Spheroids with a radius of ~100 μm, greater than the 55-70 μm range of ^{211}At α-particles, were used. Hyperthermia at 42°C for 1 hr was evaluated as a means of increasing mAb penetration into the spheroid, with the goal of improving the homogeneity of radiation dose deposition. This heating protocol was selected because it was not cytotoxic to the spheroids.   Time to reach 25 times initial volume was used as the endpoint for tumor growth delay. This volume was reached in 8.7 days in the groups incubated for 1 hr at both 37°C and 42°C without mAb. A significant regrowth delay (median ± 95% confidence interval) was achieved at activity concentrations as low as 125 kBq/ml {10.9(9.9-12.0) days at 37°C; 10.5(9.6-11.4) days at 42°C}. At 250 kBq/ml, a 25-fold increase in spheroid volume required 14.8(13.2-16.5) days at 37°C and 16.0(14.3-17.9) days at 42°C. No significant increase in cytotoxicity was seen for groups receiving hyperthermia compared with normothermic controls. Spheroids were incubated with ^{125}I-labeled chimeric 81C6, sectioned and autoradiographs were obtained to determine whether hyperthermia increased the penetration of mAb into the spheroids. Even after 4 hr heating at 42°C, the radiolabeled mAb was largely confined to the outer layers of the spheroid. We believe that this behavior reflects the limited diffusion of intact mAb as a consequence of its large size. One approach to minimizing this problem is the use of lower molecular weight constructs such as those proposed in this grant application.

Radiotoxicity of [^{211}At]astatide and ^{211}At-labeled Chimeric 81C6

One of the impediments to the evaluation of ^{211}At-labeled compounds in patients is the lack of information concerning the acute, subacute and chronic toxicities of these potential therapeutic agents. Because deastatination *in vivo* can occur, gaining an understanding of the toxicity of [^{211}At] astatide is an important step in the development of ^{211}At-labeled therapeutic agents such as mAbs and mAb fragments. With this goal in mind, we have investigated the toxicity and established the LD$_{10}$ (dose that killed 10% of exposed animals) of intravenously administered [^{211}At]astatide in two murine models. Three dose escalation experiments were performed in groups of 10 B6C3F$_1$ mice

(the standard strain used by the National Toxicology Program for carcinogenesis testing) and one dose escalation experiment was carried out in BALB/c (*nu/nu*) mice (the strain used in our laboratory for biodistribution and radiotherapy protocols). Animal weights were monitored daily and all autopsies were performed within 12 hr of death.

In B6C3F$_1$ mice, the LD$_{10}$ (with 95% confidence interval) at 365 days was 15.1 μCi (5.2-19.1 μCi) per animal, equivalent to 0.76 μCi/g (28 kBq/g) body weight. A 37.8% weight loss relative to saline controls ($P < 0.001$) was observed. The LD$_{10}$ in BALB/c (*nu/nu*) mice was 7.7 μCi (0-14.2 μCi) per animal, equivalent to about 0.35 μCi/g (13 kBq/g). High [^{211}At]astatide doses in B6C3F$_1$ mice were associated with thyroid ablation, severe bone marrow depression, testicular atrophy, focal alopecia, and nuclear atypia of the epidermoid mucosa of the fore-stomach. At activity levels approximating the LD$_{10}$, mild changes in the heart, liver and stomach were observed at 360 days; similar effects were seen in the group of BALB/c (*nu/nu*) mice receiving 10 μCi of [^{211}At]astatide.

We next initiated an investigation of the toxicity of ^{211}At-labeled chimeric 81C6 in B6C3F$_1$ mice. Because the pragmatic motivation of these studies was to provide data in support of an Investigational New Drug application, we sought the advice of the FDA on the design of the toxicity protocols. Although the first clinical studies of ^{211}At-labeled chimeric 81C6 will involve non-intravenous routes (intrathecal, neoplastic meningitis; intracystic, surgically created glioma resection cavity), it was decided to administer the labeled mAb intravenously to represent the worst possible case scenario of total leakage of activity from the injection site into the blood pool. A dose-finding experiment was performed in which groups of 10 mice received either saline or 14, 29, 63, or 110 kBq/g of ^{211}At-labeled chimeric 81C6. All of the animals in the high-dose group died between 5 and 8 days, while no deaths were observed in any other group over the 50-day observation period, suggesting a maximum tolerated dose of 63-110 kBq/g.

A second toxicity study was carried out at four dose levels in groups of 30 animals per group, each containing 15 males and 15 females. Male groups received saline or 15, 16, 51 or 81 kBq/g of ^{211}At-labeled chimeric 81C6; females received saline or 16, 17, 55 or 83 kBq/g of labeled mAb. Five mice per sex (total of 10) were terminated at 6 months and examined pathologically, and the remaining animals were followed for one year after injection. Survival studies in the 6-month groups showed no deaths in any of the female groups. In the males, 1/5 animals receiving 82 kBq/g died on day 9; all other animals remained alive. In female mice followed for 1 year, 5/10 mice died in the 83 kBq/g group (range, 69 to 309 days), 1/10 died at 55 kBq/g on day 330, and 1/10 died when treated with 16.9 kBq/g on day 216. There were no deaths in mice treated with 15.6 kBq/g or saline. In the males, 4/9 mice treated with 81 kBq/g died (range, 73 to 164 days), and 1/10 mice treated with 16.2 kBq/g died on day 296. There were no deaths in mice treated with 51 kBq/g, 14.9 kBq/g or saline. A preliminary analysis of these data suggest that the LD$_{10}$ for ^{211}At-labeled chimeric 81C6 is greater than 50 kBq/g for females and even higher for males. These results suggest that the toxicity of the ^{211}At-labeled mAb in this mouse strain is about half that of free [^{211}At]astatide. All animals received a complete autopsy within 12 hr of death. Sections of tissue from the heart, liver, lungs, kidney, spleen, testes or ovaries, thyroid, stomach, small and large intestine, and bone marrow were obtained. Comprehensive histological analysis of the tissue samples from all 150 animals are currently underway.

Preparation, Purification and Evaluation of scFv 81C6

We have successfully engineered, expressed and purified a single-chain Fv (scFv) for 81C6 anti-tenascin mAb. In order to engineer this molecule, DNA fragments encoding the variable region cDNA for the heavy- and light-chains were obtained by PCR amplification of oligo-dT primed poly(A^{1+}) tail of mRNA from the 81C6 hybridoma cell line. cDNA for the V_H and V_L regions of 81C6 were ligated via the linker sequence GGC GGA GGG GGA TCC GGT GGT GGC GGA TCT GGA GGT GGC GGC AGC which encodes the peptide sequence (Gly_4-Ser)$_3$. The PCR-primers had additional sequences including those for a linker, a stop codon, and restriction sites. Moreover, we constructed primers in such a way that tyrosine, lysine, histidine and cysteine residues could be added at the tail region. Tyrosine and lysine residues were included to facilitate radiohalogenation, cysteine residues to help in producing divalent forms of scFv, and a histidine tail to aid in further purifying the scFv with (Ni^{2+}) affinity chromatography.

The 81C6 scFv was expressed and produced in *E. coli* strain BL21(λDE3). Expression of recombinant antibody fragments in bacteria is advantageous because with this approach, large quantities of cloned gene products can be generated in relatively short time periods, at low cost, and with homogenous quality. We employed a secretion strategy for the production of 81C6 because it simplified the purification of the fragment in an active form. The 81C6 scFv protein purified by a combination of affinity chromatography and gel-filtration by HPLC, had a molecular weight of 28 kDa. Its purity was confirmed by gel filtration chromatography using a TSK 2000SW column and by SDS-PAGE.

Initial attempts to measure the binding affinity of 81C6 scFv were performed in an inhibition assay using D-247 MG cells and chimeric 81C6 as the competitor; unequivocal specific binding of the scFv could not be demonstrated. Studies are underway to determine the binding of 81C6 scFv before and after labeling using our newly developed assay (described in Methods section) which utilizes fibronectin domains 6-12 of tenascin coupled to magnetic beads. In addition, We are also currently employing an alternative approach using the *in vitro* redox-shuffling refolding protocol (Buchner *et al.*, 1992) to denature and renature the recombinant scFv protein.

Implications of 81C6 scFv Structure for Radiolabeling

Because the major goal of this project involves radiolabeling 81C6 scFv, it is important to avoid loss of antigen binding capacity due to substitution of the label in the hypervariable regions (CDRs) of the molecule which are vital for antigen recognition. The vast majority of approaches for labeling proteins with metal or halogen radionuclides involve substitution on the ϵ-amino group of lysine residues, while direct iodination methods substitute the iodine *ortho* to the hydroxyl group on tyrosine residues. With intact mAbs, a knowledge of the position and accessibility of these amino acids generally is not needed because the large number of constituent lysines and tyrosines makes the probability of modifying a critical residue relatively low. For example, chimeric 81C6 IgG has a total of 94 lysines and 58 tyrosines, and there are a sufficient number of lysines and tyrosines outside the CDRs that it can be labeled using either SIB or Iodogen and maintain an immunoreactive fraction greater than 80%. Of the tyrosines in chimeric 81C6, 20% are in the CDRs and 46% are in the variable regions as a whole; for lysines, these percentages are lower, 6% and 27%, respectively. The percentages of tyrosines and lysines observed in the CDRs

for chimeric 81C6 are similar to those reported for another chimeric mAb, HuM195 (23.3% tyrosines, 6.3% lysines).

Compared with intact mAbs, the smaller size of scFv molecules increases the probability that radiolabeling will occur in the CDR regions because lysines with high reactivity may not be available in other regions of the molecule. The number and location of the lysine and tyrosine residues in 81C6 scFv was determined by examining its amino acid sequence. As summarized in **Table 3**, the 81C6 V_H chain contains 5 lysines in the framework regions (FR) and 2 in CDR2, while the V_L chain has 3 lysines in the FRs and 1 in CDR1. If one assumes that all 11 lysines are equally available for labeling and that substitution in the CDR destroys binding to tenascin, then the maximum immunoreactivity expected would be 8/11 or about 73%. Likewise, the 81C6 V_H chain contains 3 tyrosines in the FRs and 4 in CDRs, while the V_L chain has 4 tyrosines in the FRs and 2 in CDR1. If one assumes that all 13 tyrosines are equally available for labeling and that substitution in the CDR destroys binding to tenascin, then the maximum immunoreactivity expected for direct iodination would be 7/13 or about 54%.

It is not likely that all tyrosines and lysines have the same reactivity for modification, and their relative reactivity will be dependent in large part on their accessibility to solvent. A three-dimensional model of the 81C6 Fv structure was obtained by comparison with the structure of the Fv domain of McPC603. Deletion and mutation of appropriate amino acid residues was performed using the molecular graphics program GEMM (unpublished, supplied by Dr. B.K. Lee at the NIH) run on a Silicon Graphics Indigo workstation. The sequence alignment scheme used to find corresponding residues was that of Kabat. As expected for a hydrophilic amino acid, all of the lysines on 81C6 Fv, including those in the CDRs, appear to be exposed and available for labeling. The effect of radiolabeling on the immunoreactivity and affinity of 81C6 scFv is not known at this time. If major improvements in the binding of lower molecular weight anti-tenascin constructs is required, two approaches which will be investigated are the addition of a lysine-rich tail and site-directed mutagenesis.

Table 3. **The position of lysine and tyrosine residues in 81C6 scFv**

	Lysine Position	Lysine Number	Tyrosine Position	Tyrosine Number
Heavy chain				
CDR1		0	32	1
CDR2	59,65	2	50,60	2
CDR3		0	107	1
FR1	13,19,23	3	27	1
FR2	38	1		0
FR3	66	1	79,93	2
FR4		0		0
Light chain				
CDR1	27	1	37,39	2
CDR2		0		0
CDR3		0		0
FR1		0		0
FR2	44	1	41,54	2
FR3		0	86,87	2
FR4	102,1062			0

## Identification of 81C6 Binding Epitope on Tenascin

The long-term objective of this work is to develop mAbs with higher affinity binding to the same epitope on the tenascin molecule responsible for 81C6 binding. Identification of the constituent amino acids of this epitope will allow the synthesis of peptides which then can be utilized as immunogens, ultimately leading to the generation of higher affinity, anti-tenascin, scFv by phage display technology. Because mAb 81C6 reactivity has been localized to the tenascin fibronectin 12 domain (TnFn12), the 91 amino acid sequence of TnFn 12 [EAEPEVDNLL VSDATPDGFR LSWTADEGVF DNFVLKIRDT KKQSEPLEIT LLAPERTRDL TGLREATEYE IELYGISKGR RSQTVSAIAT T] was synthesized on activated nitrocellulose as decapeptides, overlapping by eight amino acid residues, by SPOTS™ technology. Membranes, once generated, were probed with murine mAb 81C6, an irrelevant IgG$_{2b}$ murine control mAb, or buffer alone, followed by horseradish peroxidase-conjugated goat anti-mouse immunoglobulin, and developed with the ECL enhanced chemiluminescence detection system (Amersham Life Science, Arlington Heights, IL). Densitometric analysis of films was performed using the Optimas 6.0 Image Analysis system (Vashaw Scientific, Norcross, GA), with inverse grey scale values corrected for background binding with irrelevant and secondary antibodies.

The results presented below are representative of those obtained in three separate assays. Analysis of eight amino acid overlapping decapeptides revealed a cluster of positive reactivity for peptides 9-12, with a single "hot spot" of reactivity for peptide 34. The peptides so recognized contain the common sequence WTADEG, with the greatest binding occurring to peptide 12 [WTADEGVFDN]. Binding to peptide 9 [WTAD] was approximately half that observed to10-12. This suggested a minimum epitope of WTADEG with optimal binding, possibly including VFDN. That the latter is not sufficient for binding, and that WT is required for binding, is indicated by the lack of binding to peptides 13 and 14. The reactivity detected for spot 34 (TEYEIELYGI) is apparently unrelated to the reactive cluster at spots 9-12, and is unsupported by any reactivity in neighboring (33, 35) spots, suggesting an irrelevant (non-variable region binding) attachment by 81C6. As a result of this analysis, the following peptides were synthesized to determine their capacity to inhibit the binding of mAb 81C6 to native tenascin: pep 10 (WTADEG-SGGL-biotin), minimal epitope; pep 12 (WTADEGVF-SGGL-biotin), pep 14 (RLSWTADEGVFDNF), and pep 14 c (RLSWTADEGVFDNGC). Pep 10 and 12 contained the presumed inert linker SGGL for biotin conjugation, and pep 14 c contained a carboxyl-terminal cysteine to allow coupling to KLH for eventual immunization. Pep 14 represented the optimal binding peptide as determined in SPOTSscan, extending 3 amino acids towards the amino terminus and one amino acid toward the carboxyl terminus. In addition, the irrelevant 14-mer peptide (LEEKKGNYVVTDHC, pep-3) was investigated.

The ability of SPOTSscan-identified peptides to inhibit the binding of 81C6 was assayed. Relevant peptides were commercially synthesized and conjugated to BSA by coincubation of 0.5 mg peptide with 1.3 mg BSA in 0.01 N Na0H, with the pH adjusted to 7.0 with 0.1 N HCl. Glutaraldehyde (100 µl, 0.25% solution) was added and the reaction allowed to proceed for 2 hr at room temperature. The reactivity of chimeric mAb 81C6 for cell-elaborated tenascin was determined by standard radioimmunoassay (CS-RIA). The 50% endpoint concentration for H80

clone 3-elaborated tenascin was determined to be 0.5 µg/ml in this assay. This concentration of chimeric 81C6 then was exposed to a series of either free or BSA-bound synthetic peptides in increasing molar amounts (10, 40, 100, or 400 µM peptide concentration) overnight at 4°C. Absorbed, mock-absorbed (chimeric 81C6 absorbed with identical amounts of carrier BSA) and unabsorbed control chimeric 81C6 then were assayed for binding to cell-elaborated tenascin by CS-RIA. The percent inhibition of binding of mock or unabsorbed chimeric 81C6 binding was calculated. Two assays were performed with H80 clone 3 monolayers; similar results were obtained in two assays with D-247 MG monolayers.

Optimal inhibition of chimeric 81C6 binding (56-64%) was obtained with pep 14, either free or BSA-bound at a concentration of 400 µM. Lower levels of inhibition were obtained with 100 µM pep 14 or pep 14-BSA, and 400 µM pep 12-BSA. Absorption with pep 10-BSA (400 µM) resulted in minimal absorption of activity. Absorption with carrier BSA, pep 14 containing a carboxyl-terminal cysteine (pep 14C), or irrelevant pep 3 in free or bound form did not inhibit chimeric 81C6 binding. This analysis suggests that the linear peptide sequence contained in pep 14
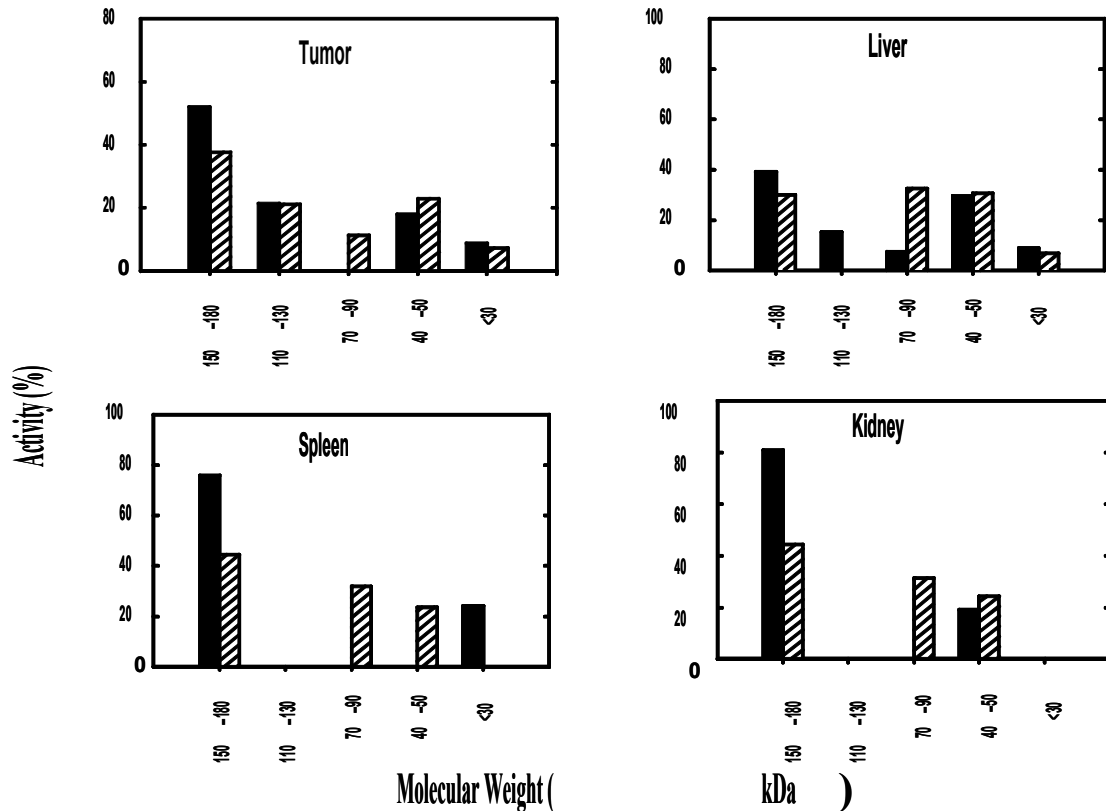

successfully competes for chimeric 81C6 binding to cell-elaborated tenascin; addition of a carboxyl terminal cysteine destroys the inhibitory activity. The greater inhibitory capacity of the longer peptide in both free and bound form, and the partial inhibition obtained with pep 12-BSA, suggests that conformational or topographical factors are important for the binding of mAb 81C6 to tenascin.

Catabolism of Murine and Chimeric 81C6 mAbs

Molecular engineering offers the possibility of selecting mAb constant region domains which are most appropriate for a particular application. Most chimeric mAbs that have been labeled with radionuclides were originally developed for other purposes, primarily antigen-dependent cell-mediated and complement-mediated cytotoxicity. For this reason, these chimeric mAbs were constructed with IgG$_1$ or IgG$_3$ constant regions because of the need for high F$_c$-receptor binding (~1 × 10^9 M^{-1}). On the other hand, binding to F$_c$ receptors is not advantageous for labeled mAbs because it could lead to increased accumulation in normal tissues such as liver and spleen. Because the affinity of human IgG$_2$ for F$_c$ receptors is negligible, an anti-tenascin chimeric mAb was produced by combining the variable region genes of murine 81C6 with human IgG$_2$ constant region domains. The specificity and affinity of this chimeric mAb were identical to those of its murine parent.

Unlike IgG$_1$ and IgG$_3$ chimeric mAbs, the tissue distribution of chimeric 81C6 was considerably different from that of its murine counterpart in several unexpected respects. Retention of radioiodine activity in subcutaneous and intracranial xenografts was significantly higher for the chimeric mAb when labeling was performed using Iodogen, with the chimeric uptake advantage reaching a factor of two at 48 hr after injection. Particularly at later time points, retention of activity in some normal tissues and blood also was higher for the chimeric construct. To determine whether the enhanced tumor localization of the chimeric construct was related to a specific process, the tumor localization index (defined as the ratio of specific to control mAb in tumor normalized to the same ratio in blood) was measured. The tumor localization index for radioiodinated chimeric 81C6 increased from 3.3 ± 0.4 at 12 hr to 127 ± 36 on Day 16 for chimeric 81C6, indicating that its tumor uptake was highly specific. Murine and chimeric 81C6 were then labeled with *N*-succinimidyl 3-iodobenzoate (SIB), a reagent previously demonstrated to increase
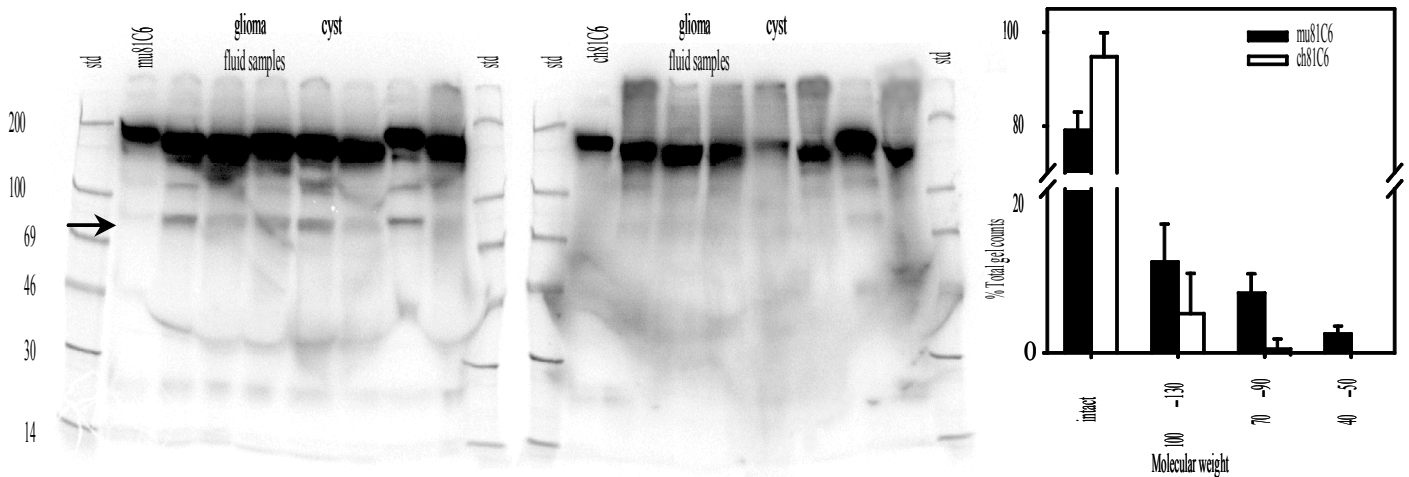
tumor localization and resistance to deiodination compared with mAb labeled using Iodogen. Labeling with SIB instead of Iodogen lowered thyroid accumulation of chimeric 81C6 by only about 5- to 17-fold, compared with a factor of as much as 108 for murine mAb. Furthermore, when both mAbs were labeled using SIB, the tumor delivery advantage conferred by the chimeric construct was not observed. Taken together, these results suggested that the catabolic processing of the two mAbs might be different.

Differences in the catabolism of radioiodinated chimeric and murine 81C6 could account for the enhanced retention of the chimeric mAb in tumor and some normal tissues. To investigate this hypothesis, the catabolism of chimeric and murine 81C6, both labeled using Iodogen, was compared in athymic mice bearing subcutaneous D-54 MG glioma xenografts. Animals were killed 1 to 6 days after injection of the mAbs, and tumor, liver, spleen and kidney were homogenized. Homogenate supernatants and blood were analyzed for trichloroacetic acid (TCA) solubility to measure the levels of low molecular weight catabolites. The percentage TCA-soluble radioactivity was <10% for both mAbs in all assays; however, less non-protein associated activity was found for the chimeric mAb in most samples. At 24 hr, TCA-soluble percentages in tumor ($1.5 \pm 0.5\%$ vs. $9.3 \pm 4.6\%$), liver ($0.8 \pm 0.3\%$ vs. $3.1 \pm 0.6\%$), spleen ($1.7 \pm 0.6\%$ vs. $4.7 \pm 0.4\%$), kidney ($0.9 \pm 0.2\%$ vs. $3.0 \pm 0.6\%$) and blood ($0.5 \pm 0.1\%$ vs. $0.9 \pm 0.1\%$) were significantly lower ($P < 0.05$) for chimeric 81C6, consistent with a lower degree of catabolism of this mAb compared with murine 81C6.

Figure 1. Distribution of radioiodinated catabolites in D-54 MG human glioma xenograft, liver, spleen and kidney 24 hr after intravenous injection of ^{131}I-labeled chimeric (black bars) and ^{125}I-labeled murine 81C6 anti-tenascin mAbs.

SDS-PAGE followed by quantitative phosphor image analysis was performed to investigate the nature of the catabolites generated *in vivo*. In tumor, 52% of the chimeric 81C6 counts at 24 hr were present in a band corresponding to intact IgG, compared with 38% for murine 81C6 **(Figure 1)**; by 144 hr, the percentage of radioactivity in tumor found as intact mAb for the chimeric mAb was more than twice that of murine 81C6. A higher percentage of radioiodine activity also was present as intact IgG for the chimeric mAb in liver, spleen and kidneys. A 70-90

kDa catabolite was observed in high abundance for murine mAb but not for chimeric mAb in tumor and normal tissues. The molecular weight of this species is consistent with the cleavage of inter-chain disulfide bonds in the murine mAb, yielding an Fab-F_c monomer.

In order to get a preliminary indication of whether the enhanced stability of the chimeric 81C6 construct would offer a practical benefit in our radioimmunotherapy trials, an *in vitro* assay was performed in which radioiodinated murine and chimeric 81C6 were incubated with tumor cyst fluid. Tumor cyst fluid was obtained from the surgically created tumor resection cavities of 7 recurrent glioma patients immediately prior to administration of ^{131}I-labeled 81C6 . The samples were sterile filtered, and stored at -170°C until needed. After a 4 hr incubation at 37°C of radioiodinated chimeric and murine 81C6 with the tumor cyst fluid, 94.7 ± 5.1% of the radioactivity remained as intact IgG for chimeric 81C6 compared with only 79.2 ± 3.8% for murine 81C6 **(Figure 2)**. In addition, levels of the 70-90 kDa catabolite (indicated on gel by arrow) were considerably higher with murine mAb. These results suggest that the chimeric construct is more inert to proteolytic degradation than its murine counterpart. We hypothesize that differences in the hinge region between the two proteins may be partially responsible for the higher stability of chimeric 81C6. This is supported by the lower flexibility of the human IgG_2 constant region compared with that of murine IgG_{2b}, and studies showing that greater hinge region rigidity can decrease solvent accessibility of regions of the IgG molecule to proteases .

Figure 2. SDS-PAGE of ^{125}I-labeled murine (left) and chimeric (center) 81C6 after incubation for 4 hr at 37°C with cyst fluid from 7 glioma resection cavity patients; quantitative analysis (right); arrow indicates 70-90 kDa catabolite.

Radiotoxicity of Intravenously Administered ^{211}At-Labeled Chimeric 81C6 mAb

Only limited information has been available concerning the acute, subacute and chronic toxicities of ^{211}At-labeled compounds, and this has been one of the major impediments to their clinical evaluation. With that goal in mind, we investigated the radiotoxicity of ^{211}At-labeled chimeric 81C6 in $B6C3F_1$ mice using protocols designed based on advice from the FDA. This strain was selected because it is the standard strain used by the National Toxicology Program for carcinogenesis testing. Although our intended clinical studies with ^{211}At-labeled mAbs all involve non-intravenous delivery routes, the labeled mAb was given intravenously to represent the worst possible case scenario of total leakage of activity from the injection site into the blood pool.

After an initial dose-finding experiment, a second toxicity study was carried out at four activity levels in 30-animal groups, each containing 15 males and 15 females. Male groups received saline or 15-81 kBq/g of ^{211}At-labeled chimeric 81C6, and females received saline or 16-83 kBq/g of labeled mAb. Five mice of each sex were terminated at 6 months and examined pathologically, and the remaining animals were followed for one year. Animal weights were monitored daily, and all autopsies were performed within 12 hr of death. The LD_{10} for intravenously administered ^{211}At-labeled chimeric 81C6 was 46 kBq/g in females and 102 kBq/g in males. Toxic effects, represented by marrow suppression, splenic white pulp atrophy, and spermatic maturational delay, were confined to rare animals receiving the highest activity levels of ^{211}At-labeled chimeric 81C6. Extrapolation of the LD_{10} values to the 70-kg standard male and the 58-kg standard female yielded LD_{10} for intravenously administered ^{211}At-labeled chimeric 81C6 of 192 mCi and 72 mCi, respectively. The differences in LD_{10} for the sexes is not known at this time.

Table 4. Residence Times for At-211 Labeled Species

Tissue	Residence time (hr)	
	^{211}At-labeled chimeric	[^{211}At]astatide
Liver	0.49	0.17
Spleen	0.04	0.05
Lungs	0.25	0.12
Heart	0.09	0.02
Kidneys	0.19	0.10
Sm. Intestine	0.25	0.31
Stomach	0.13	0.67
Blood	2.49	0.17

Our results indicate that the acute radiotoxicity of intravenously administered ^{211}At-labeled chimeric 81C6 in the B6C3F$_1$ mouse strain was about half that of [^{211}At]astatide (McLendon et al., 1996).   This observation seems counterintuitive given the relatively slow clearance of intact mAbs from most normal tissues following intravenous administration. Using previously published tissue distribution data (Garg et al., 1990; Zalutsky et al., 1997), the residence time (cumulative activity concentration in organ divided by the total activity administered) for both ^{211}At-labeled chimeric 81C6 and [^{211}At]astatide was calculated.   As summarized in **Table 4**, the residence time for ^{211}At-labeled mAb was greater than [^{211}At]astatide in liver, lungs, heart, kidneys, and blood, comparable in spleen, and less in both the stomach and small intestine.

The difference in residence time for the two labeled compounds is consistent with the fact that gastric changes were not found with labeled mAb but were observed in previous long-term

evaluations of the radiotoxicity of [^{211}At]astatide. On the other hand, the lower toxicity of ^{211}At when coupled to mAb would not be predicted based on the longer residence time for labeled mAb in most normal tissues, particularly blood. Because of the short range of α-particles in tissue, the homogeneity of radiation dose deposition could be a critical factor. The diffusion coefficient in tissue for an intact mAb such as ^{211}At-labeled chimeric 81C6 has been calculated to be 6.3×10^{-9} cm/sec, about 1,000 times higher than that for a small molecule such as [^{211}At]astatide. Given the 7.2 hr half life of ^{211}At, this slower diffusion would suggest that the toxic effects of ^{211}At-labeled mAb might be confined to regions within a few μm of vascular structures. Blood pool is generally considered to be a source organ for the calculation of marrow dosimetry. Thus, it was surprising that the threshold for marrow toxicity with ^{211}At-labeled chimeric 81C6 was higher than that seen previously with [^{211}At]astatide even though the residence time in blood for the labeled mAb was about 15 times higher. Because of the short range of α-particles in tissue, the distribution of decay sites on a cellular level becomes important in determining marrow dosimetry. In order to better understand the toxic effects of ^{211}At-labeled compounds, we propose to determine their distribution within critical organs at the histologic or cellular level, and then calculate pertinent microdosimetric parameters.

Astatine-211-Labeled Chimeric 81C6 Cytotoxicity and Microdosimetry

The geometry in which α-particle cytotoxicity is assessed is a critical parameter due to their short range in tissue. Because of our clinical interest in treating neoplastic meningitis, which presents as a thin layer of cells, a microcolony model was utilized in an attempt to simulate the geometry of this disease. The *in vitro* cytotoxicity of ^{211}At-labeled chimeric 81C6, reactive with an extracellular matrix protein, was compared to that of ^{211}At-labeled chimeric Me1-14, reactive with a cell membrane antigen, as well as to ^{211}At-labeled chimeric TPS3.2, a nonspecific control mAb. All 3 chimeric mAbs have human IgG$_2$ constant region domains and they were labeled using *N*-succinimidyl 3-[^{211}At]astatobenzoate. Microcolonies were generated from the D-247 MG human glioma and SK-MEL-28 human melanoma cell lines. The geometrical arrangement of the irradiated cells and the sites of decay relative to the cell nucleus were determined so that microdosimetry calculations could be performed. D-247 MG microcolonies contained an average of 16 cells with an average intercellular distance of 22 μm; cell and nuclear diameters were 18.5 and 9.5 μm. SK-MEL-28 cells grew in closely-packed microcolonies containing an average of 25 cells, with average cell and nuclear diameters of 20.3 and 10.7 μm, respectively. Microcolonies were incubated with ^{211}At-labeled mAbs for 1 hr, washed to remove free mAb, and incubated for an additional 23 hr. In parallel, the uptake and washout kinetics of the labeled mAbs in the microcolonies was measured to provide cumulative activity concentration data for the microdosimetry calculations. Incubations were done at mAb excess to simulate conditions likely to be encountered in patient treatment protocols.

Table 5. Calculated average absorbed dose to the cell nucleus, D_{37}, cell sensitivity value, z_0, average number of hits, $\langle n \rangle_{37}$, and fraction of cells with zero hits $P(z = 0)$, at a survival fraction of 0.37

mAb	D-247 MG cells				SK-MEL-28 cells			
	D_{37} (Gy)	z_0 (Gy)	$\langle n \rangle_{37}$	$P(z = 0)$	D_{37} (Gy)	z_0 (Gy)	$\langle n \rangle_{37}$	$P(z = 0)$

81C6	0.27	0.10	1.16	0.31	0.27	0.14	1.54	0.22
Me1-14	0.24	0.05	1.06	0.35	0.29	0.16	1.62	0.20
TPS3.2	0.28	0.09	1.20	0.30	0.29	0.15	1.55	0.21
Average	0.26	0.08	1.14	0.32	0.28	0.15	1.57	0.21

With all 3 mAbs, there was a linear decrease in survival with increasing media activity concentration and no evidence for a shoulder at low activity concentrations, consistent with the high LET of ^{211}At α-particles. Using the geometries described above and Monte Carlo transport of α-particles, the single event frequency distribution $f_1(z)$ was calculated. As shown in **Table 5**, differences in z_0, the intrinsic radiation sensitivity per traversal, for the two cell lines (D-247-MG, 0.08 ± 0.03 Gy; SK-MEL-28, 0.15 ± 0.01 Gy) were consistent with cell geometry dependent differences in specific energy distribution. For ^{211}At-labeled 81C6, reduction in survival to 37% was achieved with an average of 1.16 and 1.54 hits to the cell nucleus for D-247 MG and SK-MEL-28 microcolonies, respectively, while for ^{211}At-labeled Me1-14, these values were 1.06 and 1.62, respectively. These results demonstrate the exquisite cytotoxicity of ^{211}At-labeled mAbs in both microcolony models.

Another set of experiments was done to evaluate the cytotoxicity of ^{211}At-labeled chimeric 81C6 in spheroids formulated from the D-247 MG human glioma cell line. In order to monitor the potential effect of mAb diffusion on cytotoxic effectiveness, the radius of the spheroids, 100 μm, was greater than the range of ^{211}At α-particles. Incubations were done at both 37ºC and 42ºC for 1 hr. Under this geometry, the lowest activity at which a significant growth delay occurred was 125 kBq/ml, a value more than twice the D_{37} measured for this cell line in microcolony geometry. Autoradiography was done to investigate the rate of penetration of the mAb into the spheroid; as expected for a molecule of this size, only limited penetration into the spheroid occurred even under hyperthermic conditions. This supports the use of lower molecular weight, more rapidly diffusing molecules such as those proposed in this application, as carriers for use in tandem with ^{211}At.

Production of Astatine-211-Labeled Chimeric 81C6 for Clinical Use

Although a strong rationale has existed for some time for initiating clinical trials with ^{211}At-labeled compounds, patient studies had been impeded by the lack of appropriate methodologies for producing clinically relevant levels of ^{211}At-labeled radiopharmaceuticals. There are two aspects to this problem. First, cyclotron targetry and ^{211}At purification systems are needed to provide large quantities of ^{211}At (greater than 50 mCi) in appropriate chemical form for chemical manipulation. And second, the development of labeling and purification procedures that are appropriate for high-level syntheses under conditions where radiolytic decomposition may play a role are required. We have developed procedures which have been implemented for the production of clinical levels of ^{211}At-labeled mAbs. These methodologies have permitted the initiation of the first clinical trial of a ^{211}At-labeled endoradiotherapeutic agent, ^{211}At-labeled human/mouse chimeric anti-tenascin 81C6 mAb. A total of 16 batches of ^{211}At-labeled chimeric 81C6 have been prepared for clinical use, 12 of which were administered to glioma resection cavity patients. Three additional runs were successful; however, they were not administered because of clinical complications. The last run yielded a preparation with acceptable quality

control characteristics; however, insufficient [211]At-labeled mAb was available for injection because of the retention of high activity levels in the reaction vessel.

Table 6. Production and distillation of [211]At for clinical studies

Run	Beam Current (μA)	Irradiation Time (min)	Target Activity (mCi)	Distilled Activity (mCi)	Distillation Yield (%)
1	52	90	60	36	72
2	52	90	53	34	79
3	51	120	76	41	69
4	55	120	82	49	71
5	55	120	89	39	61
6	53	120	78	40	74
7	52	120	93	39	67
8	57	180	127	75	66
9	53	180	123	74	75
10	50	240	143	98	88
11	60	240	144	74	71
12	50	180	121	58	74
13	55	240	178	91	68
14	55	270	174	101	73
15	55	240	172	83	64
16	55	240	143	61	68

Astatine-211 was produced at the Duke University Medical Center cyclotron by bombarding natural bismuth metal targets with 28.0-MeV α-particles using the ^{209}Bi$(\alpha, 2n)^{211}$At reaction. The MIT-1 internal target system specifically designed for the production of [211]At was used. A detailed description of the target plate and modified distillation system, as well as associated methods, is presented in the Experimental Design and Methods Section. These [211]At production runs utilized beam currents of 50-60 μA α-particles and irradiation times of 1.5 to 4.5 hr (**Table 6**) with a mean yield of 0.75 ± 0.07 mCi/μA-hr. No significant differences were observed in [211]Atproduction as a function of beam current or irradiation time. The maximum level of [211]At which was produced was 178 mCi after a 4-hr irradiation at 55 μA. The decay-corrected distillation yield was $67 \pm 16\%$.

Synthesis of *N*-succimimidyl 3-[[211]At]astatobenzoate (SAB) was begun between 5 and 40 minutes after the end of the distillation, depending on whether the [211]At production was performed during the day, or for the longer duration runs, beginning at midnight. SAB was prepared by reacting in a glass vial the [211]At in chloroform, *N*-succinimidyl 3-(tri-*n*-butyl-stannyl)benzoate, *tert*-butylhydroperoxide, and glacial acetic acid. Instead of purifying SAB by HPLC, a

modification of our previously described silica gel Sep-Pak™ cartridge method was used. The pH of a 10 mg aliquot of chimeric 81C6 was adjusted to a final pH of 8.8-9.2 by the addition of saturated borate buffer in a 1:1 volume ratio. The mAb was transferred to the vial containing SAB and incubated at room temperature for 15 min. The reaction was terminated by the addition of 0.2 M glycine in borate buffer. The ^{211}At-labeled chimeric 81C6 was purified by size-exclusion chromatography using a gas-sterilized, 1.5 × 10 cm borosilicate glass chromatography column loaded with Sephadex G-25.

Yields for the synthesis of the SAB, which eluted in the 30% ethyl acetate in hexane fractions, averaged 54 ± 10%. The mean fraction of activity eluted in the hexane and 8% ethyl acetate in hexane fractions, presumably representing an At° species and an astatinated π-complex with the tin precursor aromatic ring, was 7 ± 3% and 27 ± 8%, respectively. The mean activity retained on the column, most likely in the form of [^{211}At]astatide, was 12 ± 6%. The radiation dose deposited in the chloroform solution prior to initiation of the synthesis ranged from 12,500 to 394,300 cGy, and the dose delivered during the reaction ranged from 60,350 to 159,600 cGy. Because of the potential for radiolytic effects on the radioastatodestannylation reaction, the correlation between these radiation absorbed doses and SAB yield was investigated. There was no correlation between SAB yield and the radiation dose received by the reaction mixture. No correlations were found between the radiation dose delivered prior to and during the reaction and the fraction of activity either retained on the cartridge or eluted in the hexane, 8% ethyl acetate in hexane or 30% ethyl acetate in hexane fractions.

The radiolabeling yield for the coupling of SAB to chimeric 81C6 was 76 ± 8% after a 20 min reaction at room temperature. The radiation dose to the reaction medium ranged from 399 to 1196 Gy, and there was no significant correlation between radiation dose and coupling yield. The fraction of the ^{211}At activity in the clinical preparations that was protein associated, determined by methanol precipitation, was 98.5 ± 1.0%. The fraction of ^{211}At activity which eluted with a retention time corresponding to intact IgG on size-exclusion HPLC was 96.0 ± 2.5%, with the remainder present as either aggregates (3.1 ± 2.5%) or low molecular weight impurities (0.9 ± 1.2%). All preparations had a pyrogen level <0.125 EU/mL and were determined to be sterile. After correcting for nonspecific binding, the average immunoreactive fraction for these 16 preparations was 83.3 ± 5.3%. When the immunoreactive fraction was plotted as a function of the
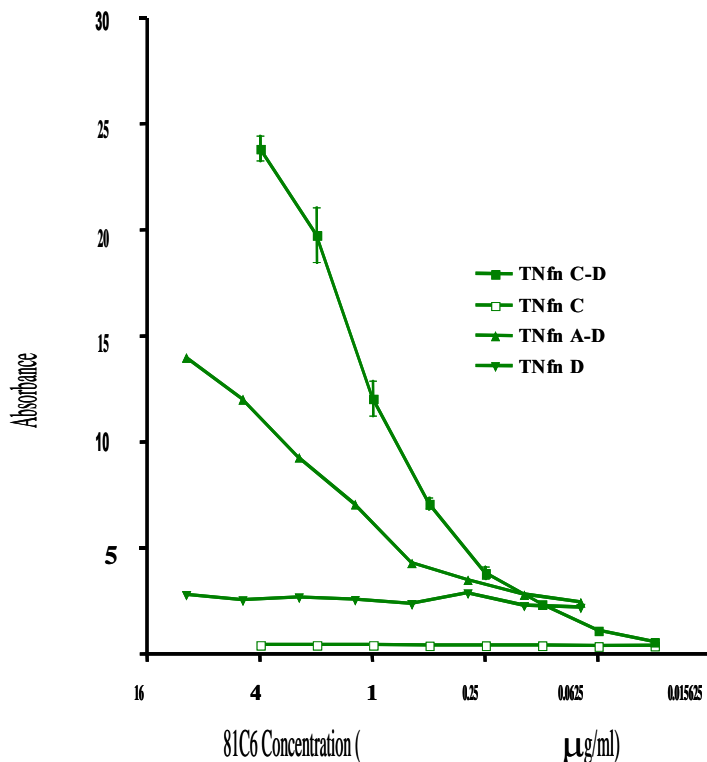
23

radiation dose received by the mAb during radiolabeling and purification, regression analysis indicated that these data were best fit by the following equation: Immunoreactive fraction = 90.8% -0.010 × radiation dose (Gy). However, this slight decrease in immunoreactivity with increasing radiation dose was not a significant effect (r^2 = 0.29).

In summary, methods and procedures have been developed for the production of high levels of ^{211}At and for the preparation of sufficient ^{211}At-labeled chimeric 81C6 to permit clinical evaluation of this promising therapeutic radiopharmaceutical. We are working on further refinements of these methodologies to increase the available activity of ^{211}At-labeled mAb per mCi ^{211}At produced, and reduce total synthesis and purification time. Nonetheless, using our current methods, we have demonstrated for the first time that it is feasible to produce sufficient levels of ^{211}At-labeled compounds to perform endoradiotherapeutic investigations in patients.

Astatine-211-Labeled Chimeric 81C6 Phase I Trial in Brain Tumor Resection Cavity Patients

Based in large part on the preclinical studies funded by this grant, we were granted an Investigational New Drug Permit in 1998 for the first clinical evaluation of a ^{211}At-labeled endoradiotherapeutic agent. The purpose of this Phase I trial is to determine the MTD and objective responses for ^{211}At-labeled chimeric 81C6 administered into SCRC of recurrent malignant glioma patients. At-211 offers several advantages for malignant glioma therapy. First, ^{211}At α-particles have a tissue range of only a few cell diameters and are much more cytotoxic than ^{131}I or ^{90}Y β-particles. And second, patient isolation is minimized due to the short half life and lack of energetic gamma emissions for ^{211}At. The ^{211}At-labeled chimeric 81C6 preparations were synthesized as described above, and immunoreactivity was confirmed prior to injection into the SCRC. All patients were given potassium iodide beginning 2 days prior to mAb treatment.

To date, 12 patients (11 GBM, 1 anaplastic oligodendroglioma) have received a single injection of 10 mg of mAb labeled with escalating doses of ^{211}At. Four were treated at our staring dose of 2 mCi, three at 4 mCi, four at 6.7 mCi, and one at 10 mCi. Serial blood sampling and gamma camera imaging were done over the next 24 hours to determine ^{211}At pharmacokinetics. Leakage of ^{211}At activity from the cavity was slow, with a mean biological half time of 763 hr, resulting in 99.1 ± 0.9% of ^{211}At decays occurring within the SCRC. Blood pool levels were only 0.032 ± 0.025% and 0.258 ± 0.432% of the injected dose at 2 and 24 hours, respectively **(Table 7)**. Clearance of ^{211}At-labeled chimeric 81C6 from the SCRC was considerably slower and leakage into the blood pool was significantly lower compared with ^{131}I-labeled murine 81C6. There have been no dose-limiting hematologic, neurologic or other toxicities associated with this treatment. The post-treatment survival range for this Phase I study has been 15 to 117 weeks, with 7 of 12 patients surviving for more than 1 year. Four patients are still alive and being followed 72, 96, 111, and 117 weeks after their treatment. Calculated radiation doses to the SCRC interface have been estimated to be between 12,400 and 78,500 cGy, with less than 5 cGy received by normal brain, liver, spleen and bone marrow. In this, the first clinical evaluation of a ^{211}At-labeled therapeutic agent, we have demonstrated that it is feasible to produce clinical levels of ^{211}At, and administer ^{211}At-labeled chimeric 81C6 mAb with minimal toxicity, very high tumor-to-normal organ dose ratios, and encouraging survival. Because of these encouraging results, we decided to evaluate the pharmacokinetics of ^{131}I-labeled chimeric 81C6 in SCRC patients. Although this has delayed further accrual in the ^{211}At-labeled chimeric 81C6 protocol, we felt that it was important to

determine the pharmacokinetics of ^{131}I-labeled chimeric 81C6 in order to be able to select the better 81C6 construct for the pivotal Phase III ^{131}I study.

Table 4. Astatine-211 blood pool activity in patients following administration of [211]At-labeled chimeric 81C6 into surgically created tumor resection cavity

Patient*	% Total Blood Pool (Decay Corrected)	
	2 hr	24 hr
1	0.006	0.060
2	0.083	0.066
3	0.033	0.463
6	0.033	0.249
7	0.009	0.052
8	0.008	0.029
9	0.046	1.424
10	0.019	0.038
11	0.060	0.160
12	0.022	0.039

*Blood samples not available from Patient s Number 4 and 5

Evaluation of ^{131}I-Labeled Chimeric 81C6 in Patients with Surgically Created Glioma Resection Cavities

The results of the biodistribution and catabolism experiments described in preceding sections of this proposal demonstrate that the chimeric 81C6 is more stable than murine 81C6 both in the presence of human tumor cyst fluid and in athymic mice bearing human glioma xenografts. In order to determine whether this enhanced stability would translate into a practical advantage in our clinical radioimmunotherapy trials, we are investigating the pharmacokinetics, dosimetry and toxicity of ^{131}I-labeled chimeric 81C6 administered into the tumor resection cavity of glioma patients. To date, a total of 23 patients have been studied, starting at the ^{131}I activity levels determined to be the MTD for murine 81C6 in recurrent (100 mCi) and newly-diagnosed (120 mCi) arms.

Table 8. Comparison of ^{131}I-labeled chimeric and murine 81C6 in glioma resection cavity patients

	Chimeric	Murine
SCRC half life	213 hr	134 hr
Blood pool half life	378 hr	70 hr
Bone marrow dose	1.19 cGy/mCi	0.41 cGy/mCi

25

In **Table 8**, the phamacokinetics and bone marrow radiation dose for ^{131}I-labeled chimeric were compared with those measured previously for murine 81C6. Consistent with its greater *in vitro* stability in the presence of tumor resection cavity fluid, the clearance of ^{131}I from the SCRC for chimeric 81C6 was slower than that measured previously for its murine counterpart. The SCRC residence times calculated for chimeric and murine 81C6 were 79 and 101 hr, respectively, indicating that the dose to the SCRC per mCi administered activity was 28% higher for chimeric 81C6. Although use of the chimeric mAb reduced the rate of leakage of ^{131}I from the SCRC, the activity which was released into the blood pool cleared much more slowly. The biological half time for chimeric 81C6 was an average of about 16 days, a value similar to that reported for human IgG$_2$. As a result of the more prolonged retention of the chimeric mAb in the blood, the radiation absorbed dose received by the bone marrow increased nearly threefold. Consistent with these results was the observation of Grade III or Grade IV hematological toxicities in about two thirds of these patients, a problem that was rarely encountered in patients receiving ^{131}I-labeled murine mAb.

From a practical perspective, the increased retention of chimeric mAb in the SCRC should be advantageous because less ^{131}I would be required, reducing cost, and the same tumor dose could be achieved with less exposure to personnel. In addition, use of ^{131}I-labeled chimeric 81C6 should make the treatment more convenient and cost effective by shortening the time that the patient must be isolated in a lead-lined room. On the other had, this would only be possible if strategies could be devised which could exploit the longer SCRC retention time while minimizing bone marrow toxicity. This has led us to pursue the development of fragments of chimeric 81C6 which contain the IgG$_2$ hinge region domains but lack CH$_2$ and possibly other domains. In this way, we hypothesize that it will be possible to retain the stability imparted by the IgG$_2$ hinge in a molecule which clears more rapidly from the blood pool.

Identification of 81C6 Binding Epitope

Knowledge concerning the nature of the epitope on the tenascin molecule responsible for 81C6 binding will facilitate the development of higher affinity mAbs and fragments with the same epitope specificity. For example, a peptide mapping the binding epitope could be used as an immunogen for generating higher affinity mAbs using phage display technology. Previous studies had suggested that the binding epitope for 81C6 was exclusively on Domain D, one of the alternatively spliced fibronectin Type III repeats; however, when the recombinant tenascin Domain D fragment (TNfn D) was used as an immunogen, only a modest immune response was obtained in mice immunized with this protein. We have now evaluated the epitope reactivity of 81C6 on the tenascin molecule using the recombinant tenascin fragments TNfn A-D, TNfn A-C, TNfn C-D, TNfn C, and TNfn D and both ELISA and Western Blotting.

Figure 3. Analysis of 81C6 binding to recombinant tenascin fragments by ELISA

ELISA was performed against tenascin or the recombinant tenascin fragments by coating 96 well plates with 50 µl of 4 µg/ml of each protein in 0.1 M carbonate buffer, pH 9.6. Plates were incubated overnight at 4°C and rinsed with 115 mM phosphate buffer (pH 7.4), 0.05% BSA and 0.05% Brij 35. Fifty microliters of murine 81C6 or isotype-control mAb (45.6) dilutions were added to triplicate wells and incubated for 1 hr at room temperature. Plates were rinsed with the above buffer, 50 µl (1 µg/ml) of biotinylated rabbit anti-mouse IgG was added per well, and incubated for 30 minutes at room temperature. After rinsing, 50 µl of streptavidin-alkaline phosphatase was added per well and incubated for 30 minutes. Plates were rinsed and 100 µl of substrate was added per well. The substrate was 200 mM Tris buffer with 0.005M $MgCl_2$ and 4 mg/ml *p*-nitrophenyl phosphate. Color was developed for 10-20 minutes at room temperature and stopped by the addition of 50µl of 20 mM L-cysteine in deionized water. Absorbancy was read in a plate reader at a wavelength of 405 nm.   The results, summarized in **Figure 3**, clearly demonstrate that both the C and D alternatively spliced fibronectin Type III repeats must be present in order to form the binding epitope for 81C6.

Western Blotting was performed by adding 1-2 µg of tenascin or tenascin fragment to each lane of a 4-20% polyacrylamide gradient gel. Proteins were reduced with 25 mM DTT in sample buffer by boiling for 5 minutes prior to loading on to the gel. After electrophoresis, protein bands were transferred to 0.22 µm nitrocellulose paper using a Bio-Rad semi dry blotter. The paper was blocked overnight by soaking in 5% (w/v) milk in 115 mM phosphate buffer. After blocking, the paper was rinsed with 115 mM phosphate buffer with 0.05% BSA and 0.05% Brij 35, and then the blot was soaked for one hr in 1 µg/ml 81C6 or 45.6 (isotype control) diluted in the rinse buffer for 1 hr. After rinsing 4 times, the blot was soaked in 0.25 µg/ml of HRP-rabbit anti-mouse IgG for 30 minutes, and then rinsed extensively. Reactivity was detected by chemiluminescence using a SuperSignal West Pico kit (Pierce) and exposing to Kodak Biomax film for 5 to 60 seconds. Again, 81C6 reacted with tenascin, TNfnA-D, TNfn C-D but not with TNfn A-C, TNfn D, or TNfn C, indicating that 81C6 binding requires that fibronectin III domains C and D both be present.

Radioiodinated 81C6 scFv Fragment

We have engineered, expressed and purified a recombinant anti-tenascin scFv fragment for 81C6. In order to engineer this molecule, the variable region cDNA for the heavy and light chains were obtained by polymerase chain reaction (PCR) amplification of the oligo-dT primed poly(A$^+$) tail of mRNA from the 81C6 hybridoma cell line. The 81C6 scFv cDNA (V$_H$-linker-V$_L$) was constructed using the PCR method by combining the V$_H$ region sequence and V$_L$ region sequence *via* the linker sequence GGC GGA GGG GGA TCC GGT GGT GGC GGA TCT GGA GGT GGC GGC AGC which encodes the peptide (Gly$_4$-Ser)$_3$. The PCR primers had additional sequences including those for a linker, a stop codon, and hexa-histidine tag. The purpose of the histidine tail was to aid in purification of the scFv with (Ni^{2+}) affinity chromatography. The fragment was cloned into the pMR1scFv vector and the expression was done under T7 promoter control. The complete nucleotide and deduced amino acid sequence of 81C6 scFv, including heavy-chain, (Gly$_4$-Ser)$_3$ linker, light-chain, and His-tag is shown in **Figure 3**. The 81C6 scFv was expressed and produced in the *E.coli* strain BL21(λDE3).

Our initial attempts to produce and purify 81C6 scFv employed a secretion strategy because it simplifies the purification of scFv in an active form; however, the 81C6 scFv failed to fold correctly. BIAcore analysis was performed and the scFv fragment generated by this approach did not exhibit reasonable binding affinity for recombinant tenascin. We have now successfully produced an scFv fragment with good tenascin binding using a protocol consisting of metal-chelating affinity chromatography followed by *in vitro* redox-shuffling refolding to renature and purify the recombinant 81C6 scFv protein to near homogeneity as a 26 kDa monomer (Kuan et al., 2000a). The binding kinetics of 81C6 scFv to the recombinant TNfnCD fragment were analyzed by BIAcore and compared with those of chimeric 81C6. The K$_D$ for 81C6 scFv was 8.6 × 10^{-9} M, within an order of magnitude of the value measured for the bivalent intact mAb **(Table 9)**. In order to investigate its thermal stability, the scFv was then incubated at 37°C for 48 hr and its binding parameters were measured again; more than 80% of its binding affinity was maintained.

The 81C6 scFv fragment has been labeled with ^{131}I and ^{125}I in 60-70% yield and 1.8-2.7 mCi/mg specific activity using the Iodogen method. The immunoreactive fraction, measured using recombinant TNfnCD tenascin fragment coupled to magnetic beads as the antigen-positive target, was greater than 50%. Several tissue distribution studies have been performed in athymic mice bearing subcutaneous D-54 MG human glioma xenografts in order to evaluate the *in vivo* behavior of radioiodinated 81C6 scFv. In the first experiment, animals received intravenous injections of ^{125}I-labeled 81C6 scFv and as a control, ^{131}I-labeled MR-1 scFv. MR-1scFv was selected for this purpose because its isoelectric point, pI = 6.5, is similar to that of 81C6 scFv. As shown in the left panel of **Figure 10**, the tumor uptake of 81C6 scFv peaked at 6.8 ± 1.4 % ID/g and declined gradually thereafter. The specific-to-control scFv tumor uptake ratio reached 19:1 at 24 hr. A second experiment was performed in which ^{131}I-labeled anti-Tac scFv, which has a pI of 9.5, served as the control **(Figure 10,** right panel**)**, and even higher specific -to-control scFv tumor uptake ratios were observed. In the kidney, ^{125}I activity levels were 1.5 to 3.3 times higher than those for ^{131}I at 0.5 and 1 hr (81C6 scFv, 22.4 ± 2.6% ID/g; anti-Tac scFv, 76.7 ± 7.2% ID/g at 0.5 hr), suggesting that the lower isoelectric point might have helped at least transiently reduce binding to the negatively-charged renal tubule. The relatively slow clearance of 81C6 scFv from tumor was somewhat surprising and may reflect multimer formation. Catabolic studies will be performed to investigate this in detail.

Table 9. Binding of 81C6 scFv and intact mAb to TNfnCD tenascin fragment measured by BIAcore

Protein	k_{assoc} (M^{-1} sec^{-1})	k_{dissoc} (sec^{-1})	K_D (M)
chimeric 81C6 IgG	7.6×10^6	9.0×10^{-3}	1.3×10^{-9}
81C6 scFv	1.4×10^6	1.2×10^{-2}	8.6×10^{-9}
81C6scFv (37°C/4 hr)	9.1×10^5	1.0×10^{-2}	1.1×10^{-8}

V_H FR1

```
TAACTTTAAGAAGGAGATATACATATGGAGGTCCAGCTGCAGCAGTCTGGACCTGAGCTG   60
                          M   E⁺¹ V   Q   L   Q   Q   S   G   P   E   L
```
20

CDR1
```
GTAAAGCCTGGGGCTTCAGTGAAGATGTCCTGCAAGGCTTCTGGATACACATTCACTAGC   120
 V   K   P   G   A   S   V   K   M   S   C²²  K   A   S   G   Y   T   F   T   S
```
40

FR2
```
TATGTTGTGCACTGGGTGAAGCAGAACCCTGGGCAGGGCCTTGAGTGGATTGGATATATT   180
 Y   V   V   H   W³⁶  V   K   Q   N   P   G   Q   G   L   E   W   I   G   Y⁵⁰  I
```
60

FR3
```
AATCCTTTCAATGATGGTACTAAGTACAATGAGAACTTCAAAGGCAAGGCCACACTGACT   240
 N   P   F   N   D   G   T   K   Y   N   E   N   F   K   G   K⁶⁶  A   T   L   T
```
80

```
TCAGACAGATCCTCCAGCACAGCCTACATGGAGCTCAGCAGCCTGACCTCTGAGGAATCT   300
 S   D   R   S   S   S   T   A   Y   M   E   L   S   S   L   T   S   E   E   S
```
100

CDR3   FR4
```
GCGGTCTATTTCTGTGCAAGAGACATGGGTCGCGAAGGCTTTGCTTACTGGGGCCAAGGG   360
 A   V   Y   F   C⁹²  A   R   D⁹⁵  M   G   R   E   G   F   A   Y¹⁰³ W   G   Q   G
```
120

LINKER
```
ACTCTGGTCACTGTCTCTGCAGGCGGAGGGGGATCCGGTGGTGGCGGATCTGGAGGTGGC   420
 T   L   V   T   V   S   A¹¹⁴ G   G   G   G   S   G   G   G   G   S   G   G   G
```
140

$\mathbf{V_L}$ F$_R$1

GGCAGCGATATTGTGATGACGCAGGCTGCATTCTCCAATCCAGTCACTCTTGGAACATCA   480

  G   S   D^{+1} I   V   M   T   Q   A   A   F   S   N   P   V   T   L   G   T   S

160

CDR1

GCTTCCATCTCCTGCAGGTCTAGTAAGAGTCTCCTACATAGTAATGGCATCACTTATTTG   540

  A   S   I   S   C^{23} R^{24} S   S   K   S   L   L   H   S   N   G   I   T   Y   L

180

F$_R$2   CDR2

TATTGGTATCTGCAGAAGCCAGGCCAGTCTCCTCAGCTCCTGATTTATCAGATGTCCAAC   600

  Y   W^{35} Y   L   Q   K   P   G   Q   S   P   Q   L   L   I   Y   Q^{50} M   N

200

F$_R$3

CTTGCCTCAGGAGTCCCAGACAGGTTCAGTAGCAGTGGGTCAGGAACTGATTTCACACTG   660

  L   A   S   G^{57} V   P   D   R   F   S   S   S   G   S   G   T   D   F   T   L   220

CDR3

AGAATCAGCAGAGTGGAGGCTGAGGATGTGGGTGTTTATTACTGTGCTCAAAATCTAGAA   720

  R   I   S   R   V   E   A   E   D   V   G   V   Y   Y   C^{88} A^{89} Q   N   L   E   240

F$_R$4 $\mathbf{\mathit{H_{IS}-T_{AG}}}$

CTTCCTCGGACGTTCGGTGGAGGCACCAAGCTGGAAATCAAACATCATCATCATCATCAT   780

  L   P   R   T   F^{97} G   G   G   T   K   L   E   I   K^{106} H   H   H   H   H   H
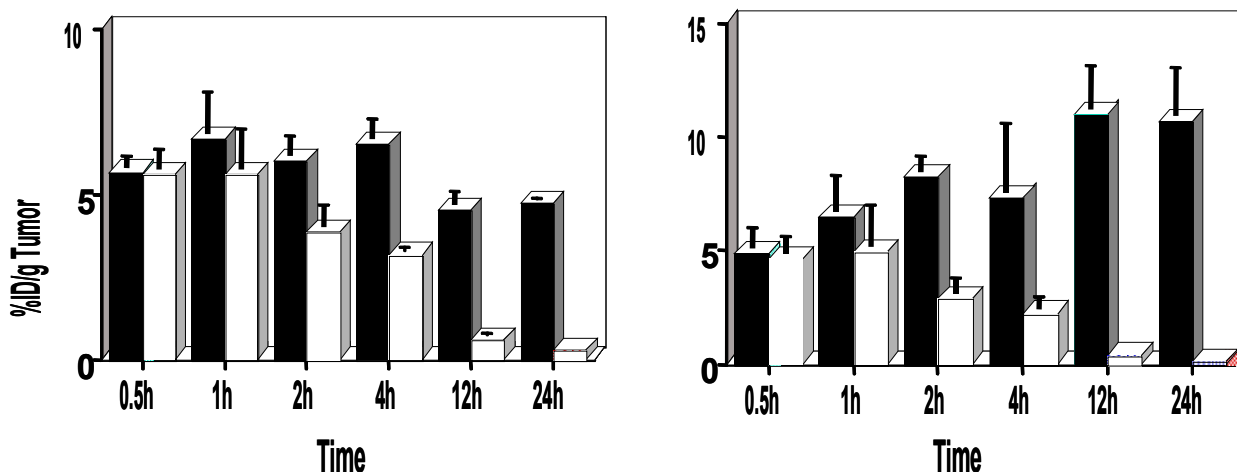
260

CATTGA

786

  C Stop

261

Figure 9. The complete nucleotide and deduced amino acid sequence for 81C6 scFv showing heavy chain, (Gly$_4$Ser)$_3$ linker, light chain, and hexa-histidine tag.

30

Figure 10. Uptake of scFv fragments in D-54 MG human glioma xenografts following intravenous injection of radioiodinated scFv fragments. Left, ^{125}I-labeled 81C6 scFv (black bars) and ^{131}I-labeled MR-1 scFv (white bars); right, ^{125}I-labeled 81C6 scFv (black bars) and ^{131}I-labeled anti-Tac scFv (white bars).

Radiolabeled Anti-Tenascin mAbs and Lymphoma

Although our clinical investigations with radiolabeled anti-tenascin mAbs to date have been limited to patients with CNS malignancies, these radiopharmaceuticals might be useful in the diagnosis and treatment of other tenascin-expressing tumors as well. We have been working with Dr. David Rizzieri in the Division of Oncology at Duke to investigate whether anti-tenascin mAbs might be of value in the treatment of non-Hodgkin's lymphomas (NHL). NHL of intermediate grade generally respond to chemotherapy; however, most relapse, and 5 year survival is only about 40%. A preliminary study was performed to determine tenascin expression in lymphoid tissue and relate its expression to microvessel density (Rizzieri et al., 1999). Tenascin expression increased concomitantly with microvessel density, consistent with the possible role of tenascin in angiogenesis.

Immunohistochemical methods were used to determine tenascin expression in biopsies obtained from 13 NHL patients. In most patients, serial biopsies were available. Our results were highly encouraging; uninvolved sites including bone marrow did not stain for tenascin, but tumor-infiltrated lymph nodes, marrow, and other tissues were positive. Furthermore, the intensity of tenascin staining increased significantly with transformation of the disease to higher grades and with progression of the disease. We have now obtained an IND (BB-IND-9124) and Institutional Review Board Approval for a clinical trial investigating the pharmacokinetics of ^{131}I-labeled chimeric 81C6 administered intravenously to NHL patients. The goal will be to determine the optimal mAb protein dose for saturating tenascin in normal liver and spleen to maximize tumor uptake as is currently done with anti-CD-20 mAbs to saturate binding to normal B-cells. In addition to differences in normal tissue binding, tenascin and CD20 differ in one other important respect. Unlike CD-20, which is primarily expressed in low-grade NHL, high-level expression of tenascin occurs in intermediate and high-grade NHL. Thus, if we are successful in developing

31

better anti-tenascin constructs, they might be of value for the radioimmunotherapy of lymphoma, particularly when used in tandem with the α-particle emitting radionuclide [211]At.

C.   PUBLICATIONS

Peer-Reviewed Journal Articles Supported Fully or Mainly by this Grant

Zalutsky, M.R., Archer, G.E., Garg, P.K., Batra, S.K., and Bigner, D.D. Chimeric anti-tenascin antibody 81C6:increased tumor localization compared with its murine parent. Nucl. Med. Biol. 1996; 23:449-458.

Hauck, M.L., Dewhirst, M.W., and Zalutsky, M.R. The effects of clinically relevant hyperthermic temperatures on the kinetic binding parameters of a monoclonal antibody. Nucl. Med. Biol., 1996; 23:551-55.

Hauck, M.L., Dewhirst, M.W., Bigner, D.D., and Zalutsky, M.R. Local hyperthermia improves uptake of a chimeric monoclonal antibody in a subcutaneous xenograft model. Clinical Cancer Res., 1997; 3:63-70.

Zalutsky, M.R., Stabin, M., Larsen, R.H. and Bigner, D.D. Tissue distribution and radiation dosimetry of astatine-211-labeled chimeric 81C6, an α-particle emitting immunoconjugate. Nucl. Med. Biol., 1997; 24:255-262.

Larsen, R.H., Akabani, G., Welsh, P. and Zalutsky, M.R. (1998) The cytotoxicity and microdosimetry of [211]At-labeled chimeric monoclonal antibodies on human glioma and melanoma cells *in vitro*. *Radiation Res.* 149:155-162.

Hauck, M.L., Larsen, R.H., Welsh, P.C. and Zalutsky, M.R. (1998) Cytotoxicity of α-particle emitting [211]At-labeled antibody in tumor spheroids: no effect of hyperthermia. *Br. J. Cancer* 77:753-759.

Larsen, R.H., Slade, S. and Zalutsky, M.R. (1998) Blocking [[211]At]astatide accumulation in normal tissues: evaluation of seven potential compounds. *Nucl. Med. Biol.* 25:351-357.

Hauck, M.L. and Zalutsky, M.R. (1998) The effects of hyperthermia on the catabolism of a radioiodinated chimeric monoclonal antibody. *Clinical Cancer Res.* 4:2071-2077.

Reist, C.J., Bigner, D.D. and Zalutsky, M.R. (1998) Human IgG_2 constant region enhances *in vivo* stability of anti-tenascin antibody 81C6 compared with its murine parent. *Clinical Cancer Res.* 4:2495-2502.

McLendon, R.E., Archer, G.E., Larsen, R.H., Akabani, G., Bigner, D.D., and Zalutsky, M.R. (1999) Radiotoxicity of systemically administered [211]At-labeled human/mouse chimeric monoclonal antibody: a long-term survival study with histological analysis. *Int. J. Radiat. Oncol. Biol. Phys.* 45:491-499.

32

Foulon, C.F., Bigner, D.D., and Zalutsky, M.R. (1999) Preparation and characterization of anti-tenascin monoclonal antibody-streptavidin conjugates for pretargeting applications. *Bioconjugate Chem.* 10:867-876.

McLendon, R.E., Archer, G.E., Larsen, R.H., Akabani, G., Bigner, D.D., and Zalutsky, M.R.: Radiotoxicity of systemically administered [211]At-labeled human/mouse chimeric monoclonal antibody: a long-term survival study with histological analysis. Int. J. Radiat. Oncol. Biol. Phys. 1999; 45:491-499.

Zalutsky, M.R. and Vaidyanathan, G.: Astatine-211-labeled radiotherapeutics: an emerging approach to targeted alpha particle therapy. Current Pharm. Design 2000; 6:1433-1455.

Zalutsky, M.R., Zhao, X.-G., Alston, K.L., and Bigner, D.D.: High-level production of α-particle-emitting [211]At and preparation of [211]At-labeled antibodies for clinical use. J. Nucl. Med. 2001; 42:1508-1515.

Boskovitz, A., Akabani, G., Pegram, C.N., Bigner, D.D., and Zalutsky, M.R.: Human/murine chimeric anti-tenascin 81C6 F(ab')$_2$ fragment: preclinical evaluation of a potential construct for the targeted radiotherapy of malignant glioma. Nucl. Med. Biol; 2004; 31:345-355.

Yordanov, A.T., Pozzi, O., Carlin, S., Akabani, G., Wieland, B., and Zalutsky, M.R.: Wet harvesting of no-carrier-added [211]At from an irradiated [209]Bi target for radiopharmaceutical applications. J. Radioanal. Nucl. Chem., 2004; 262:593-599.

Hauck, M.L. and Zalutsky, M.R.: Enhanced tumour uptake of radiolabelled antibodies by hyperthermia: Part I: Time of injection relative to hyperthermia. Int. J. Hyperthermia, 2005; 21:1-11.

Hauck, M.L. and Zalutsky, M.R.: Enhanced tumour uptake of radiolabelled antibodies by hyperthermia: Part II: Application of the thermal equivalency equation. Int. J. Hyperthermia, 2005; 21:13-27.

Pozzi, O.R. and Zalutsky, M.R.: Radiopharmaceutical chemistry of targeted radiotherapeutics II: Radiolytic effects of astatine-211 α-particles influence *N*-succinimidyl 3-[[211]At]astatobenzoate synthesis. J. Nucl. Med; 2005; 46:1393-1400.

Peer-Reviewed Journal Articles Supported In Part by this Grant

Bigner, D.D., Brown, M., Coleman, R.E., Friedman, A.H., Friedman, H.S., McLendon, R.E., Bigner, S.H., Wikstrand, C.J., Pegram, C.N., Kerby, T., and Zalutsky, M.R. Phase I studies of treatment of malignant glioma and neoplastic meningitis with ^{131}I-radiolabeled monoclonal antibodies anti-tenascin 81C6 and anti-chondroitin proteoglycan sulfate Me1-14 F(ab')$_2$ - A preliminary report. J. Neuro-Oncol. 1995; 24:109-122.

Garg, P.K., Alston, K.L., and Zalutsky, M.R. Catabolism of radioiodinated murine monoclonal antibody F(ab')$_2$ fragment labeled using *N*-succinimidyl 3-iodobenzoate and Iodogen methods. Bioconjugate Chem., 1995; 6:493-501.

Larsen, R.H., Wieland, B.W., and Zalutsky, M.R. Evaluation of an internal cyclotron target for the production of astatine-211 via the ^{209}Bi(α,2n)^{211}At reaction. Appl. Radiat. Isotop., 1996; 47:135-143.

McLendon, R.E., Archer, G.E., Garg, P.K., Bigner, D.D., and Zalutsky, M.R. Radiotoxicity of systemically administered [^{211}At]astatide in B6C3F$_1$ and BALB/c (*nu/nu*) mice: a long term survival study with histologic analysis. Int. J. Radiat. Oncol. Biol. Phys., 1996; 35:69-80.

Brown, M.T., Coleman, R.E., Friedman, A.H., Friedman, H.S., McLendon, R.E., Reiman, R., Felsberg, G.J., Tien, R.D., Bigner, S.H., Zalutsky, M.R., Zhao, X.G., Wikstrand, C.J., Pegram, C.N., Herndon II, J.E., Vick, N.A., Paleologos, N., Fredericks, R.K., Schold, Jr., S.C., and Bigner, D.D. Intrathecal ^{131}I-labeled anti-tenascin monoclonal antibody 81C6 treatment of patients with leptomeningeal neoplasms or primary brain tumor resection cavities with subarachnoid communication: Phase I trial results. Clin. Cancer Res. 1996; 2:963-972.

Zalutsky, M.R. and Bigner, D.D. Radioimmunotherapy with α-particle emitting radioimmuno-conjugates. Acta Oncologica, 1996; 35:373-379.

Vaidyanathan, G. and Zalutsky, M.R. Targeted therapy using alpha emitters. Physics Med. Biol., 1996; 41:1915-1931.

Foulon, C.F., Schoultz, B.W. and Zalutsky, M.R. Preparation and biological evaluation of an astatine-211 labeled biotin conjugate: biotinyl-3-[^{211}At]astatoanilide. Nucl. Med. Biol., 1997; 24:135-143.

Foulon, C.F., Alston, K.L. and Zalutsky, M.R. Synthesis and preliminary biological evaluation of 3-iodobenzoyl norbiotinamide and 5-iodo-3-pyridine acyl norbiotinamide: two radioiodinated biotin conjugates with improved stability. Bioconjugate Chem.; 1997, 8:179-186.

Hauck, M.L., Coffin, D.O., Dodge, R.K., Dewhirst, M.W., Mitchell, J.B., and Zalutsky, M.R. (1997) A local hyperthermia which enhances antibody uptake in a glioma xenograft model does not affect tumor interstitial fluid pressure. *Int. J. Hyperthermia* 13:307-316.

Vaidyanathan, G., Affleck, D.J. and Zalutsky, M.R. (1997) A method for the radioiodination of proteins using *N*-succinimidyl 3-hydroxy-4-iodobenzoate. *Bioconjugate Chem.* 8:724-729.

Akabani, G. and Zalutsky M.R. (1997) Microdosimetry of At-211 using histological images: application to bone marrow. *Radiation Res.* 148:599-607.

Foulon, C.F., Alston, K.L. and Zalutsky, M.R. (1998) Astatine-211 labeled biotin conjugates resistant to biotinidase for use in pretargeted radioimmunotherapy. *Nucl. Med. Biol.* 25:81-88.

Bigner, D.D., Brown, M.T., Friedman, A.H., Coleman, R.E., Akabani, G., Friedman, H.S., Thorstad, W.L., McLendon, R.E., Bigner, S.H., Zhao, X.-G., Pegram, C.N., Wikstrand, C.J., Herndon II, J.E., Vick, N.A., Paleologos, N., Cokgor, I. and Zalutsky, M.R. (1998) Iodine-131-labeled anti-tenascin monoclonal antibody 81C6 treatment of patients with recurrent malignant

gliomas: Phase I trial results. *J. Clin. Oncol.* 16:2202-2212.

Akabani, G., Reist, C.J., Cokgor, I., Friedman, A.H., Friedman, H.S., Coleman. R.E., Bigner, D.D., and Zalutsky, M.R. (1999) Dosimetry of I-131 labeled 81C6 monoclonal antibody administered into surgically created resection cavities in malignant brain tumor patients. *J. Nucl. Med.* 40:631-638.

Akabani, G., Cokgor, I., Coleman, R.E., González Trotter, D., Wong, T., Friedman, H.S., Garcia-Turner, A., Herndon, J.E. II, DeLong, D., McLendon, R.E., Zhao, X.-G., Pegram, C.N., Bigner, D.D., and Zalutsky, M.R. (2000) Dosimetry and dose-response relationships in newly diagnosed patients treated with iodine-131-labeled anti-tenascin monoclonal antibody therapy. *Int. J. Radiat. Oncol. Biol. Phys.* 46:947-958.

Cokgor, I., Akabani, G., Kuan, C.-T., Friedman, H.S., Friedman, A.H., Coleman, R.E., McLendon, R.E., Bigner, S.H., Zhao, X.-G., Garcia-Turner, A.M., Pegram, C.N., Wikstrand, C.J., Herndon II, J.E., Provenzale, J.M., Zalutsky, M.R., and Bigner, D.D.: Phase I trial results of ^{131}I-labled anti-tenascin monoclonal antibody 81C6 treatment of patients with newly diagnosed malignant gliomas. J. Clin. Oncol. 2000; 18:3862-3872.

Reardon, D.A., Akabani, G., Coleman, R.E., Friedman, A.H., Friedman, A.H., Herndon II, J.E., Cokgor, I., McLendon, R.E., Pegram, C.N., Provenzale, J.M., Quinn, J.A., Rich, J., Regalado, L.V., Sampson, J.H., Shaffman, T.D., Wikstrand, C.J., Wong, T.Z., Zalutsky, M.R., and Bigner, D.D.: Phase II trial of murine ^{131}I-labeled anti-tenascin monoclonal antibody 81C6 administered into surgically created resection cavities of patients with newly diagnosed malignant gliomas. J. Clin. Oncol. 2002; 20:1389-1397.

Akabani, G. McLendon, R.E., Bigner, D.D., and Zalutsky, M.R.: Vascular targeted endoradiotherapy using alpha-particle emitting compounds: theoretical analysis. Int. J. Radiat. Oncol. Biol. Phys. 2002; 1259-1275.

Carlin, S., Mairs, R.J., Welsh, P., and Zalutsky, M.R.: Sodium-iodide symporter (NIS)-mediated accumulation of [[211]At]astatide in NIS-transfected human cancer cells. Nucl. Med. Biol. 2002; 29:729-739.

Akabani, G., Kennel, S.J., and Zalutsky, M.R.: Microdosimetric analysis of alpha particle emitting targeted radiotherapeutics using histological images. J. Nucl. Med., 2003; 44:792-805.

Carlin, S., Akabani, G. and Zalutsky, M.R.: Cytotoxicity of [[211]At]astatide and [^{131}I]iodide to glioma tumor cells in vitro expressing the sodium iodide symporter (NIS). J. Nucl. Med. 2003; 44: 1827-1838.

Rizzieri, D.A., Akabani, G., Zalutsky, M.R., Coleman, R.E., Metzler, S.D., Bowsher, J.E., Toaso, B., Anderson, E., Lagoo, A., Clayton, S., Pegram, C.N., Moore, J.O., Gockerman, J.P., DeCastro, C., Gasparetto, C., Chao, N.J., and Bigner, D.D.: Phase I trial of ^{131}I-labeled chimeric 81C6 monoclonal antibody for the treatment of patients with non-Hodgkin's lymphoma. Blood 2004; 104:642-648.

35

Akabani, G., Reardon, D.A., Coleman, R.E., Wong, T.Z., Metzler, S.D., Bowsher, J.E., Barboriak, D.P., Provenzale, J.M., Greer, K.L., Delong, D., Friedman, H.S., Friedman, A.H., Zhao, X.-G., Pegram, C.N., McLendon, R.E., Zalutsky, M.R., and Bigner, D.D.: Dosimetry and radiographic analysis of iodine-131-labeled anti-tenascin 81C6 murine monoclonal antibody in newly diagnosed patients: a phase II study. J. Nucl. Med, 2005; 46:1042-1051.

Reardon, D.A., Akabani, G., Coleman, R.E., Friedman, A.H., Friedman, H.S., Herndon II, J.E., McLendon, R.E., Pegram, C.N., Provenzale, J.M., Quinn, J.A., Rich, J.N., Vredenburgh, J., Desjardins, A., Guruangan, S., Badruddoja, M., Dowell, J., Wong, T.Z., Zhao, X.-G., Zalutsky, M.R., and Bigner, D.D.: Salvage radioimmunotherapy with murine ^{131}I-labeled anti-tenascin monoclonal antibody 81C6 for patients with recurrent primary and metastatic malignant brain tumors: Phase II study results. J. Clin. Oncol. 2006; 24:115-122.

Boyd, M., Ross, S.C., Dorrens, J., Fullerton, N.E., Tan, K.W., Zalutsky, M.R., and Mairs, R.J.: Radiation induced biological bystander effect elicited *in vitro* by targeted radiopharmaceuticals labeled with $\alpha-$, $\beta-$ and Auger Electron emitting radionuclides. J. Nucl. Med. 2006; 47:1007-1015.

Reardon, D.A., Zalutsky, M.R., Akabani, G., Coleman, R.E., Friedman, A.H., Friedman, H.S., Herndon II, J.E., McLendon, R.E., Pegram, C.N., Bohlin, C.W., Provenzale, J.M., Quinn, J.A., Rich, J., Sampson, J.H., Gururangan, S., Shafman, T.D., Wikstrand, C.J., Wong, T.Z., Zhao, X.-G., and Bigner, D.D.: Phase I trial of ^{131}I-labeled human/mouse chimeric anti-tenascin monoclonal antibody 81C6 administered into surgically created resection cavities of patients with malignant gliomas. J. Nucl. Med. 2006; 47:912-918.

Vaidyanathan, G., Alston, K.L., Bigner, D.D. and Zalutsky, M.R.: N^ϵ-(3-[*I]iodobenzoyl)-Lys^5-N^αmaleimido-Gly^1-GEEEK ([*I]IB-Mal-D-GEEEK): A radioiodinated prosthetic group containing negatively charged D-glutamates for labeling internalizing monoclonal antibodies. Bioconjugate Chem. 2006; 17:1085-1092.

Vaidyanathan, G. and Zalutsky, M.R.: *N*-succinimidyl 3-[*I]iodobenzoate: an agent for the indirect radioiodination of proteins. Nature Protocols 2006; 1:707-713.

Book Chapters and Reviews Supported Fully or In Part by this Grant

Hauck, M.L., Dewhirst, M.W., and Zalutsky, M.R.: Enhancement of radiolabeled monoclonal antibody uptake in tumors with local hyperthermia. In: *Targeted Delivery of Imaging Agents*. Torchilin, V.P., ed., CRC Press, Boca Raton, FL, 1995; 335-361.

Zalutsky, M.R., Schuster, J.M., Garg, P.K., Archer, Jr., G.E., Dewhirst, M.W., and Bigner, D.D.: Two approaches for enhancing radioimmunotherapy: alpha emitters and hyperthermia. Recent Results Cancer Res. 1996; 141:101-122.

Bast, R.C., Jr., Zalutsky, M.R., and Frankel, A.: Monoclonal Serotherapy. In: *Cancer Medicine*, 4th edition.   Holland, J.F., Frei III, E., Bast, R.C., Jr., Kufe, D.W., Morton, D.L., and Weichselbaum, R.R., eds., Williams and Wilkins, Baltimore, 1996; 1245-1262.

Archer, G.E., Zalutsky, M.R., and Bigner, D.D.: Immunoconjugates. In: *Gliomas.* Berger, M.S., and Wilson, C., eds., W.B. Saunders Co., Orlando, 1999; 609-618.

Zalutsky, M.R.: Radiohalogens for Radioimmunotherapy.   In: *Radioimmunotherapy of Cancer.* Abrams, P.G. and Fritzberg, A.R., eds., Marcel Dekker, New York, 2000; 81-106.

Cokgor, I., Akabani, G., Wikstrand, C., Zalutsky, M.R., Friedman, H.S., and Bigner, D.D.: Radiolabeled monoclonal antibodies for malignant glioma: an improvement over current therapy? Oncology Medscape 2000; Volume 3, Issue 3.

Wikstrand, C.J., Zalutsky, M.R., and Bigner, D.D.: Therapy of brain tumors with radiolabeled antibodies. In: *Brain Tumor Immunotherapy.* Liau, L.M., Becker, D.P., Cloughsey, T.F., and Bigner, D.D., eds., Humana Press, Totowa, New Jersey 2001; 205-229.

Bast, R.C., Jr., Zalutsky, M.R., Kreitman, R.J., Sausville, E.A. and Frankel, A.: Monoclonal serotherapy. In: *Cancer Medicine*, 5th edition. Bast, R.C., Jr., Kufe, D.W., Pollock, R.E., Weichselbaum, R.R., Holland, J.F., and Frei III, E., eds., B.C. Decker, Hamilton, Ontario, 2000; 860-875.

Zalutsky, M.R. and Lewis, J.: Radiolabeled antibodies for tumor imaging and therapy.   In: *Handbook of Radiopharmaceuticals: Radiochemistry and Applications*. Welch, M.J. and Redvanly C., eds., Wiley, Chichester, United Kingdom, Wiley, Chichester, UK, 2003; 685-714.

Zalutsky, M.R.: Radionuclide therapy.   In: *Handbook of Nuclear Chemistry Volume 4: Radiochemistry and Radiopharmaceutical Chemistry in Life Sciences* Roesch, F., ed., Kluwer Academic, Dordrecht, Netherlands, 2003; 315-348.

Zalutsky, M.R.: Targeted Radiotherapy of brain tumours. Br. J. Cancer 2004; 90:1469-1473.

Zalutsky, M.R., Reardon, D.A., Akabani, G., Friedman, A.H., Friedman, H.S., and Bigner, D.D.: Targeted irradiation of brain tumours. In: *Targeted Cancer Therapies*, Bruland, O.S. and Flaegstad,T., eds., Tromso University Press, Tromso, Norway, 2003; 155-159.

Bast, R.C., Jr., Kousparou, C.A., Epenetos, A.A., Zalutsky, M.R., Kreitman, R.J., Sausville, E.A., and Frankel, A.E.: Antibodies. In: *Cancer Medicine*, 6th edition. Kufe, D.W., Pollock, R.E.,Weichselbaum, R.R., Bast, R.C., Jr., Gansler, T.S., Holland, J.F., and Frei III, E., eds., B.C. Decker, Hamilton, Ontario**,** 2003; 881-898.

Boskovitz, A., Wikstrand, C.J., Kuan, C.-T., Zalutsky, M.R., Reardon, D.A., and Bigner, D.D., Monoclonal antibodies for brain tumor treatment. Expert Opinion Biol. Therapy 2004; 4:1-19.

Zalutsky, M.R. and Pozzi, O.R.: Radioimmunotherapy with alpha-particle emitting radionuclides. Quart. J. Nucl. Med. Mol. Imaging 2004; 48:289-296.

Zalutsky, M.R.: Current Status of Therapy of Solid Tumors: Brain Tumor Therapy. J. Nucl. Med. 2005; 46:151S-156S.

Bast, R.C., Zalutsky, M.R., Kreitman, R.J. and Frankel, A.E.: Monoclonal Serotherapy. In: *Cancer Medicine*, 7th edition. Kufe, D.W., Bast, R.C., Hait, W.N., Hong, W.K., Pollock, R.E.,Weichselbaum, R.R., Gansler, T.S., Holland, J.F., and Frei III, E., eds., B.C. Decker, Hamilton, Ontario, 2006; 770-785.

Zalutsky, M.R., Pozzi, O.R., and Vaidyanathan, G.: Targeted radiotherapy with alpha particle emitting radionuclides. In: Trends in Radiopharmaceuticals, IAEA, Vienna, 2006; in press.

Zalutsky, M.R.: Potential of Immuno-positron emission tomography for tumor imaging and therapy planning. Clinical Cancer Res. 2006; 12:1958-1960.

Zalutsky, M.R.: Targeted alpha particle therapy of microscopic disease: providing further rationale for clinical investigation. J. Nucl. Med. 2006; in press.